JACS
JOURNAL OF THE AMERICAN CHEMICAL SOCIETY

ARTICLE

pubs.acs.org/JACS

Structure−Activity Relationships of GHRP-6 Azapeptide Ligands of the CD36 Scavenger Receptor by Solid-Phase Submonomer Azapeptide Synthesis

David Sabatino,[†,§] Caroline Proulx,[†] Petra Pohankova,[‡] Huy Ong,[*,‡] and William D. Lubell[*,†]

[†]Department of Chemistry and [‡]Department of Pharmacology, Université de Montréal, P.O. Box 6128, Downtown Station, Montréal QC H3C 3J7, Canada

[§]Department of Chemistry and Biochemistry, Seton Hall University, 400 South Orange Avenue, South Orange New Jersey 07079, United States

Supporting Information

ABSTRACT: The cluster of differentiation 36 (CD36) class B scavenger receptor binds a variety of biologically endogenous ligands in addition to synthetic peptides (i.e., growth hormone-releasing peptides, GHRPs), which modulate biological function related to anti-angiogenic and anti-atherosclerotic activities. Affinity labeling had previously shown that GHRP-6 analogues such as hexarelin, [2-Me-W^2]GHRP-6 (**1**), bind to the lysine-rich domain of the CD36 receptor. Moreover, the azapeptide analogue [aza-F^4]GHRP-6, **2**, exhibited a characteristic β-turn conformation as described by CD and NMR spectroscopy and a slightly higher CD36 binding affinity relative to hexarelin (1.34 and 2.37 μM, respectively), suggesting receptor binding was mediated by the conformation and the aromatic residues of these peptide sequences. Ligand-receptor binding interactions were thus explored using azapeptides to examine influences of side-chain diversity and backbone conformation. In particular, considering that aromatic cation interactions may contribute to binding affinity, we have explored the potential of introducing salt bridges to furnish GHRP-6 azapeptide ligands of the CD36 receptor. Fifteen aza-glutamic acid analogues related to **2** were prepared by submonomer solid-phase synthesis. The azapeptide side chains were installed by novel approaches featuring alkylation of resin-bound semicarbazone with Michael acceptors and activated allylic acetates in the presence of phosphazene base (BTPP). Moreover, certain Michael adducts underwent intramolecular cyclization during semicarbazone deprotection, leading to novel pyrrazoline and aza-pyroglutamate *N*-terminal residues. Structural studies indicated that contingent on sequence the [aza-Glu]GHRP-6 analogues exhibited CD spectra characteristic of random coil, polyproline type II and β-turn secondary structures in aqueous media. In covalent competition binding studies with the GHRP-6 prototype hexarelin bearing a radiotracer, certain [aza-Glu]GHRP-6 azapeptides retained relatively high (2−27 μM) affinity for the CD36 scavenger receptor.

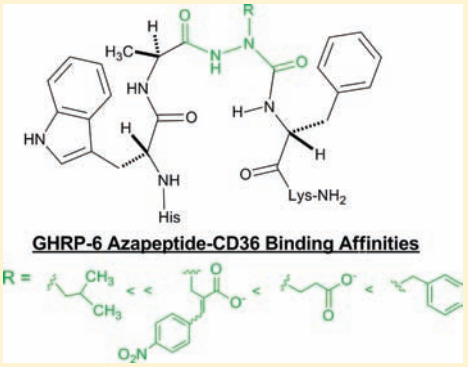

INTRODUCTION

Glutamate residues are often key structural elements for the biological activity of small molecules and peptides, because the acidic side chains may interact with target receptors by selective ionic interactions.[1−3] Moreover, constrained glutamate analogues constitute important tools for exploring biological activity at the molecular level. Such ligands may function as modulators of receptor activity with enhanced pharmacokinetic properties for potential therapeutic applications (Figure 1).[1−4,7]

Azapeptides are a class of conformationally preorganized peptide mimics (peptidomimetics) which have been shown to adopt β-turn conformations using computation, X-ray and spectroscopic analyses.[5] Substitution of the α-carbon with nitrogen rigidifies the peptide conformation because the diacyl hydrazine and urea moieties of the resulting semicarbazide constrain respectively the φ and ψ dihedral angles of the peptide backbone.[5] In bioactive sequences, aza-amino acid residues have shown improved bioavailability, receptor binding affinity and selectivity, as well as metabolic stability for potential use in therapeutic applications.[6] For example, in the rare case of glutamate replacement by aza-glutamate[333] (**4**, Figure 1), the resulting antigenic hen egg ovalbumin 325−339 azapeptide exhibited major histocompatibility complex class II (MHC II) protein binding and partial agonism, demonstrating that conservative aza-substitution at a T-cell receptor contact site could induce a minor structural perturbation sufficient to alter T-cell signaling.[4c]

In spite of a useful example of aza-Glu in studying peptide recognition,[4c] as well as successful applications of related aza-residues (i.e., aza-Gln, aza-Asp, aza-Asn) to furnish enzyme inhibitors, (Figure 1),[4,7] aza-amino acids possessing carboxylate side chains have been rarely used in structure−activity relationship

Received: August 12, 2010
Published: June 21, 2011

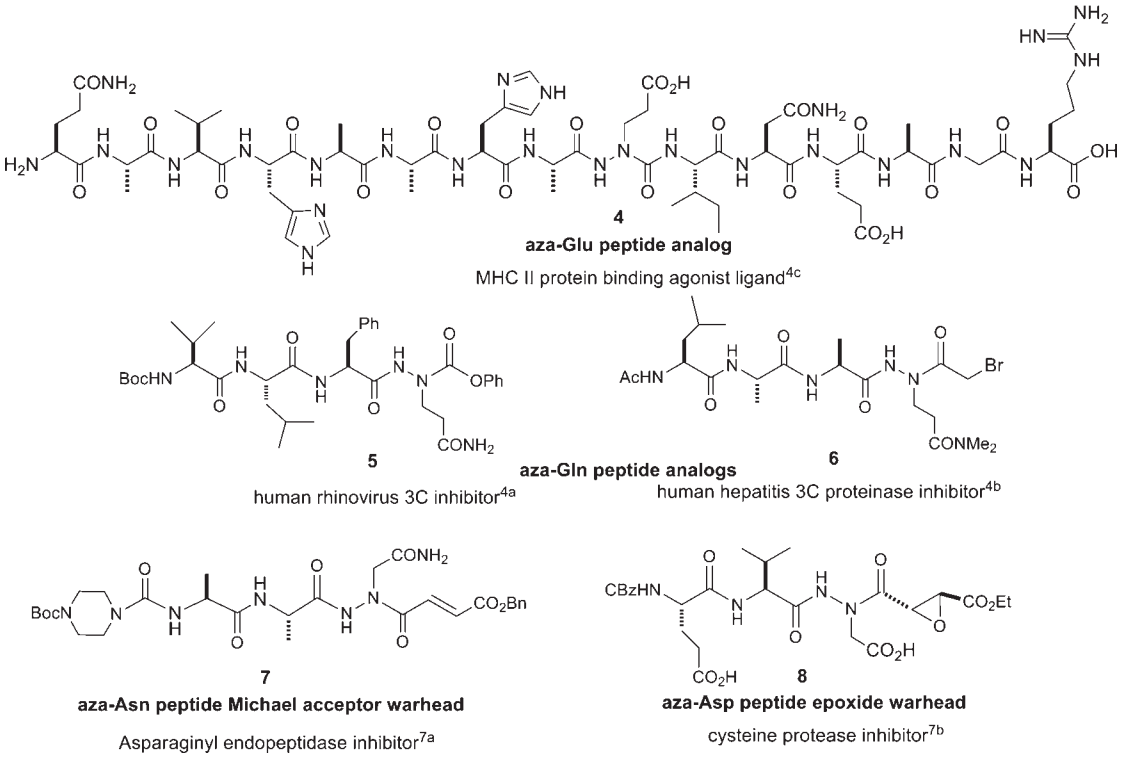

Figure 1. Bioactive azapeptide analogues bearing aza-residues with carboxylate side chains.

studies. Azapeptides bearing carboxylate side chains may bind by way of ionic interactions to induce biological activity at target receptors. However, their application has been particularly hampered due to lack of selectivity when differentiating hydrazine nitrogen atoms in solution-phase synthesis, which required separation of isomeric mixtures.[4c] Moreover, although pyroglutamate analogues of peptides have been shown to improve bioavailability and stability of active sequences, to the best of our knowledge, there have been no applications of aza-pyroglutamate analogues.[8]

The cluster of differentiation 36 (CD36) is a membrane glycoprotein member of the class B scavenger receptor family which binds among a variety of endogenous ligands, thrombospondin 1 (TSP1) an extracellular matrix protein and oxidatively modified low density lipoprotein (oxLDL).[9] This receptor ligand interaction has been found to play a major role in cardiovascular biology, with inhibitory effects in angiogenesis and in the development of atherosclerosis in hyperlipidemic states.[9,10] Growth hormone-releasing peptides (GHRPs)[11] have previously been reported as the first class of synthetic peptide derivatives, which serve as ligands of CD36 and exhibit anti-atherosclerotic activity in a CD36 dependent manner.[9c] Topographical mapping of the CD36 receptor by covalent binding using a benzophenone alanine (Bpa) analogue of hexarelin, (Tyr-Bpa-Ala-His-D-2-Me-Trp-Ala-Trp-D-Phe-Lys-NH_2) has shown that the extracellular binding domain (Asn^{132}-Gln^{177}) encompasses Lys rich residues,[12] and overlaps with the oxLDL binding domain, which features three conserved Lys residues at position 163, 164 and 166, of which two positively charged Lys residues at positions 164 and 166 directly contribute to binding.[13] Considering the structures of GHRP-6 and the Lys-rich domain of the CD36 receptor, aromatic cation interactions may be hypothesized to contribute to affinity.[14a] Recently, [aza-Phe^4]GHRP-6 (**2**) was shown to exhibit a circular dichroism (CD) spectrum indicative of a β-turn conformation and to bind discriminately to the CD36 receptor, suggesting that the aromatic character and conformation of the azapeptide contributed to binding affinity.[15a] Recognizing that salt bridges have been shown to compete with aromatic cation interactions,[14b−d] we have explored the influence of aza-Glu residues on binding affinity in GHRP-6 azapeptide ligands of the CD36 receptor.

Submonomer solid-phase synthesis was developed to provide azapeptides without hydrazine chemistry in solution.[15,16] Aza-amino acid residues were built directly onto support-bound peptide by selective alkylation of an aza-Gly residue. This method consisted of (A) acylation of peptide-bound resin with an activated benzylidene carbazate, (B) alkylation of the resulting semicarbazone and (C) deprotection followed by conventional Fmoc-based SPPS (Scheme 1).[15]

Novel alkylation chemistry featuring Michael additions of electron-deficient olefins and conjugate addition−elimination of activated allylic acetates is now reported to prepare aza-Glu azapeptides. Fifteen aza-Glu derivatives were prepared using this method to systematically modify the Ala^3 and Trp^4 positions of GHRP-6. Moreover, novel aza-pyroglutamate analogues were prepared by replacement of the His^1 residue of GHRP-6 with pyrrazoline amino acids. Structural analyses of the aza-Glu analogues by CD spectroscopy and [aza-F^4]GHRP-6 (**2**) by NMR spectroscopy, as well as CD36 receptor binding affinities were performed to assess relationships between azapeptide structure and biological activity.

RESULTS

Synthesis. Azapeptide synthesis was performed on Rink amide linker attached to Merrifield resin[17] using Fmoc-based SPPS.[18]

Scheme 1. Submonomer Solid-Phase Azapeptide Synthesis[15]

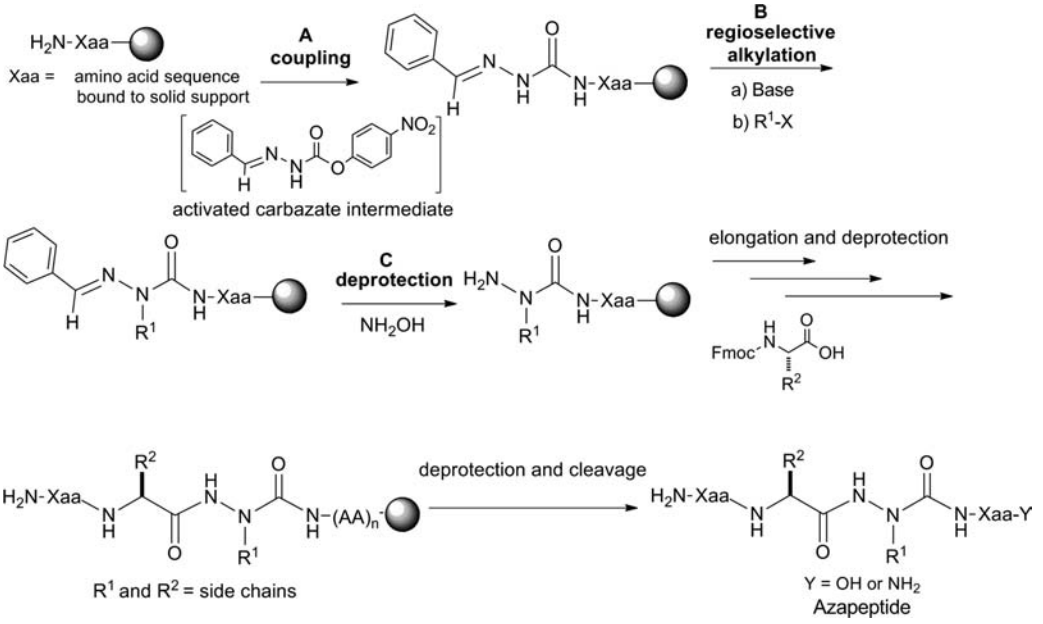

Resin-bound peptides D-Phe-Lys(Boc) **9** and Trp(Boc)-D-Phe-Lys(Boc) **23** constituted the starting sequences for making azapeptides with respective aza-modifications at the Trp[4] and Ala[3] positions of the GHRP-6 sequence. The aza-Gly residue was first installed onto supported di- and tripeptides by way of an activated benzylidene carbazate intermediate **10**, which was generated in situ from benzaldehyde hydrazone and *p*-nitrophenylchloroformate.[15]

Michael Additions. Michael addition reactions were explored on semicarbazone resins **11** and **24** to generate, respectively, aza-Glu analogues at positions Trp[4] and Ala[3], **12**−**14** and **25**−**30** (Scheme 2). *tert*-Butyl acrylate and acrylamide were employed to install side chains corresponding to aza-Glu and aza-Gln residues. Moreover, acrylonitrile, vinyl phosphonate and vinyl sulfonate Michael acceptors were employed to examine reaction scope and expand diversity. The products from addition of the vinyl phosphonate and sulfonate acceptors were also pursued because they may be converted to nonhydrolyzable surrogates of phosphate and sulfate esters of serine (or cysteine), with interesting potential for studying inhibition of enzymes that modify such residues (i.e., kinases, phosphatases and sulfatases).[19]

Semicarbazone resins **11** and **24** were swollen in THF and treated with base (potassium *tert*-butoxide or *tert*-butyliminotri(pyrrolidino)phosphorane [BTPP] 300 mol %) and Michael acceptor (300 mol %). Improved conversions and cleaner reactions were observed with the phosphazene base BTPP (29−75%) relative to potassium *tert*-butoxide (21−49%). Diethylvinyl phosphate and phenylvinyl sulfone were observed to be relatively less reactive Michael acceptors and provided resins **14**, **28** and **29** with modest conversions (29−50%) and significant recovered starting material, as indicated after resin cleavage and LCMS analyses.

To liberate the amine for further Fmoc-based peptide synthesis, semicarbazones **12**−**14** and **25**−**30** were treated with $NH_2OH \cdot HCl$ in pyridine.[15] In the case of phosphonates **13** and **27**, semicarbazone deprotection occurred with some concomitant phosphonate diester solvolysis, giving mixtures of phosphonate diester and monoester. Subsequent peptide elongation by standard SPPS[18] afforded four [aza-Glu[4]]GHRP-6 (**19**−**22**) and five [aza-Glu[3]]GHRP-6 (**36**−**40**) analogues in acceptable overall yields (4−10%) and purities (90−99%) after reverse-phase HPLC purification (Table 1, entries 4−12).

Conjugate Addition−Elimination of Activated Allylic Acetates. Glutamic acid analogues bearing an aromatic alkylidene substituent at the side-chain 4-position have exhibited biological activity in peptide sequences and small-molecule peptidomimetics.[20] 4-Alkylidene aza-glutamates were thus pursued to study the influence of the combination of an aromatic and carboxylate side chain on peptide conformation and affinity to the CD36 receptor. To procure 4-alkylidene glutamate analogues, the stereoselective alkylation of a glycine Schiff base by an activated allylic acetate had been previously explored using chiral phase transfer and transition metal catalysts, as well as auxiliaries.[21] Inspired by these procedures, uninhibited by stereochemical issues, the corresponding aromatic [4-alkylidene aza-Glu[4]]GHRP-6 derivatives were pursued by conjugate addition−elimination reactions of activated allylic acetates **48**−**51** onto semicarbazone resin **11** (Scheme 4).

Allylic acetates **48**−**51** were synthesized in racemic form by the Baylis-Hillman reaction[22] of aromatic aldehydes and electron-deficient alkenes using trimethylamine as catalyst, followed by alcohol acetylation (Scheme 3).[23] In our hands, benzaldehydes with electron-deficient *para*-substituents reacted better than their electron rich counterparts producing allylic alcohols **44**, **45** and **47** in 46−65% yields. Alternatively, *p*-methoxybenzaldehyde reacted sluggishly with acrylonitrile giving 25% isolated yield of allylic alcohol **46**, after silica gel column chromatography. Allylic acetates **48**−**51** were prepared in 47−92% yields from Baylis−Hillman adducts **44**−**47** by acetylation with acetyl chloride in a pyridine/dichloromethane solution, followed by silica gel column chromatography.[24]

Semicarbazone resin **11** was swollen in THF and exposed to conjugate addition−elimination reactions using allylic acetates **48**−**51**. Modest conversions (40−55%) were obtained with

dx.doi.org/10.1021/ja203007u |*J. Am. Chem. Soc.* 2011, 133, 12493–12506

Scheme 2. Submonomer Solid-Phase Synthesis of [aza-Glu]GHRP-6 Azapeptides[a]

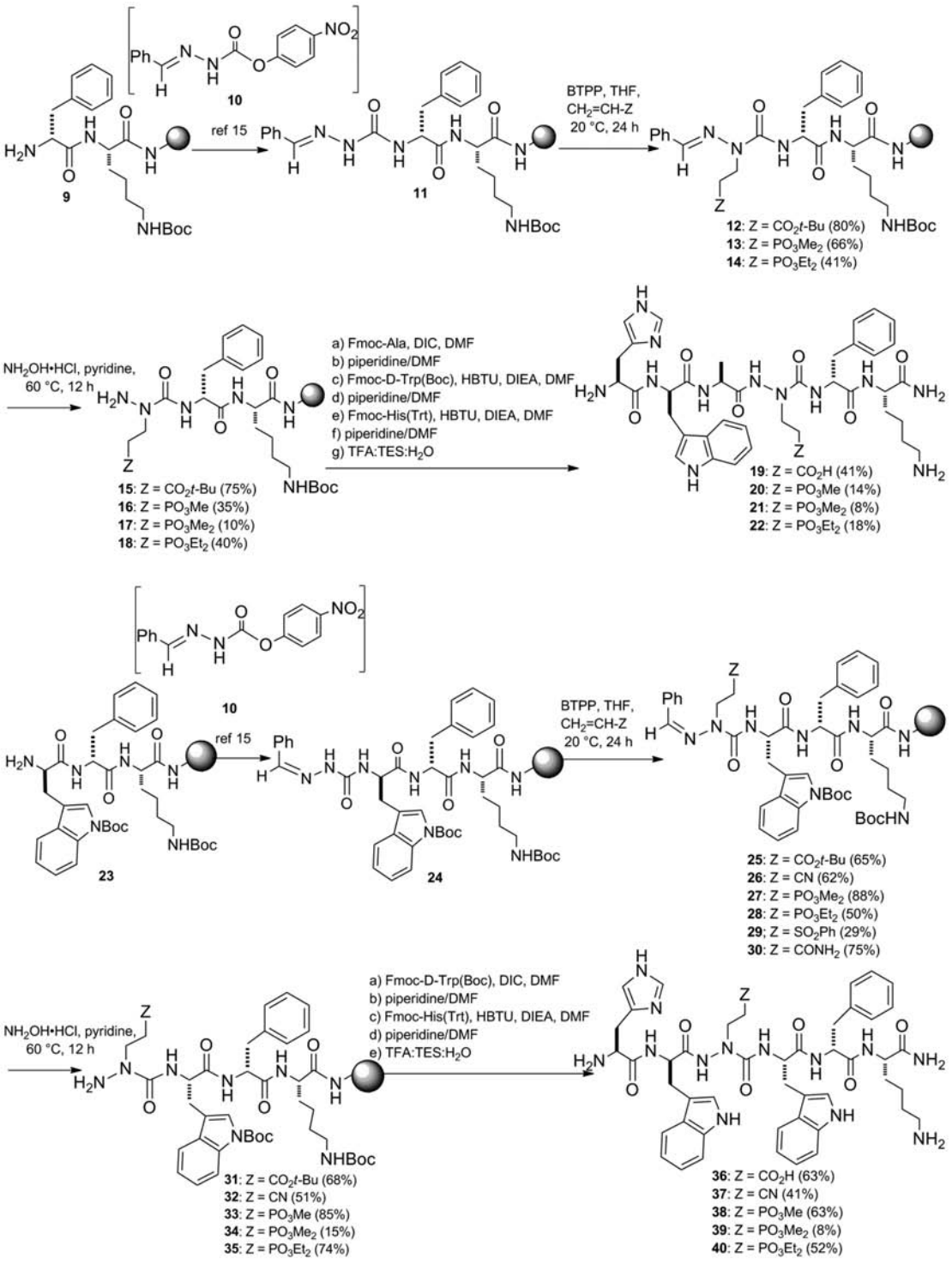

[a] Percents in parentheses refer to crude purities of peptide product as assessed after cleavage of a small aliquot of resin using TFA/H_2O/TES, followed by LCMS analysis using 0−80% MeOH in H_2O with 0.1% FA as eluant.

potassium *tert*-butoxide (300 mol %) as base with allylic acetates **48**−**51** (300 mol %) as assessed after resin cleavage and LCMS analysis. Improved conversions (58−74%) were achieved with the organic soluble, non-ionic Schwesinger base, BTPP (300 mol %),[25] which as a non-nucleophilic alternative, may avoid side reaction with the electrophile (Scheme 4).[21b] Diastereomers were attributed to 1:1 mixtures of olefin isomers *E*- and *Z*-**52**−**55**, which were apparent in LCMS analyses as separable peaks having identical masses (see Supporting Information for LCMS data).

Semicarbazones **52**−**55** were generally converted to semicarbazides using $NH_2OH \cdot HCl$ in pyridine,[15] however, semicarbazone **53**, bearing both electron deficient nitrile and *p*-nitro-cinnamyl

Table 1. Characterization Data for Azapeptides

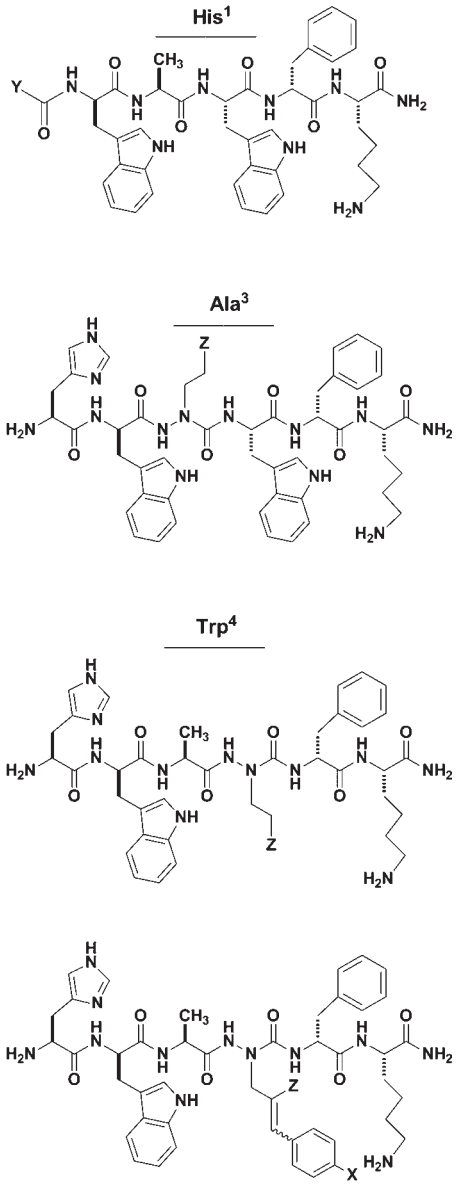

entry	azapeptide	Y	crude purity[a]	isolated yield[b]	isolated purity[c,d] RT (min)[e,f]		mass[g]
1	64	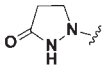	53%	9%	97% 16.7	97% 12.0	848.0(848.4)
2	65	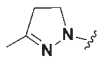	30%	8%	>99% 18.8	97% 14.0	846.0(846.4)
3	66	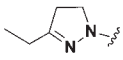	39%	8%	90% 19.4	93% 14.4	860.0(860.4)
		Z					
4	36	CO_2H	63%	10%	98% 11.3	97% 8.96	932.0(932.4)
5	37	CN	41%	5%	90% 10.7	85% 8.85	913.0(913.4)
6	38	PO_3Me	63%	6%	99% 13.7	97% 10.1	982.1(982.4)
7	39	PO_3Me_2	8%	4%	99% 11.2	98% 8.71	997.1(997.4)
8	40	PO_3Et_2	52%	4%	96% 12.2	99% 9.31	1024.1(1024.4)
9	19	CO_2H	41%	6%	92% 9.56	97% 8.59	816.0(816.4)
10	20	PO_3Me	14%	5%	92% 11.5	93% 9.46	868.1(868.2)
11	21	PO_3Me_2	8%	4%	96% 9.58	92% 8.65	881.1(881.4)
12	22	PO_3Et_2	18%	5%	99% 10.9	96% 9.12	909.0(909.4)
		Z, X					
13	56	CO_2H, NO_2	36%	9%	92% 14.3	90% 10.3	950.0(950.2)
14	57	CN, OMe	71%	12%	97% 11.8	99% 9.3	916.0(916.4)
15	58	CN, H	74%	13%	>99% 11.4	>99% 9.2	886.0(886.4)

[a] Crude purity. [b] Isolated yield calculated from resin loading. [c] Isolated purity by LCMS at 214 nm. [e] Retention times using 0−80% MeOH in H_2O (0.1% FA). [d] Isolated purity by LCMS at 214 nm. [f] Retention times using 0−80% MeCN in H_2O (0.1% FA) as eluants. [g] Expected mass (observed mass) as $[M + H]^+$ by LCMS.

moieties, gave no product after repetitive treatments and only starting material was recovered. The azapeptides **56**−**58** were subsequently completed by standard peptide synthesis in acceptable yields (9−13%) and purities (90−99%) after reverse-phase HPLC purification (Table 1, entries 13−15).

Although azapeptide **57** was observed as a single peak by analytical HPLC, its ^1H and ^{13}C NMR spectra exhibited a doubling of peaks indicative of a 3:1 *E*/*Z*-olefin ratio at 333 K. At reduced temperatures (318 and 298 K, Figure 2), additional splitting of signals observed was likely due to isomerization about the tertiary urea. The lack of exchange between the signals of the vinyl protons at 6.22 and 6.18 ppm during NOESY experiments confirmed the independence of the olefin isomers (see Supporting Information for NMR spectra of **57**). Conversely, the ^1H and ^{13}C NMR spectra of [aza-Phe[4]]GHRP-6 (**2**) at 298 K were indicative of configurationally pure azapeptide in D_2O and DMSO-d_6, as discussed below.

Aza-pyroglutamate and Aza-dehydroproline Synthesis. Under analogous conditions for semicarbazone removal, aza-Gln analogue **30** was accompanied by intramolecular amidation

Scheme 3. Preparation of Allylic Acetates via Baylis−Hillman Reaction[22]

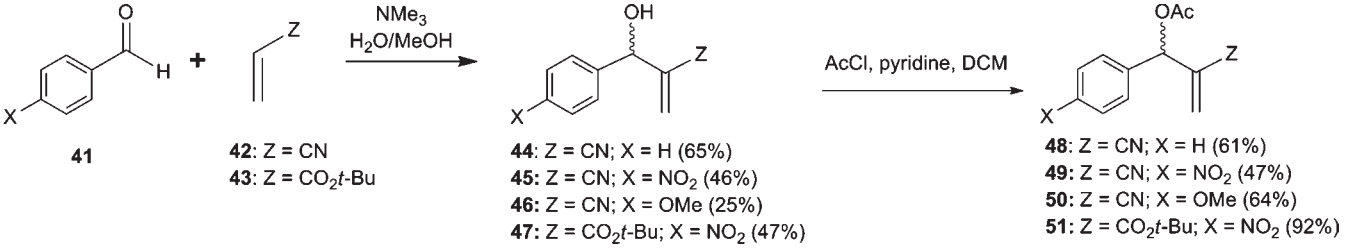

Scheme 4. Submonomer Solid-Phase Synthesis of Aromatic [4-alkylidene aza-Glu^4]GHRP-6, 56 and Analogues 57 and 58[a]

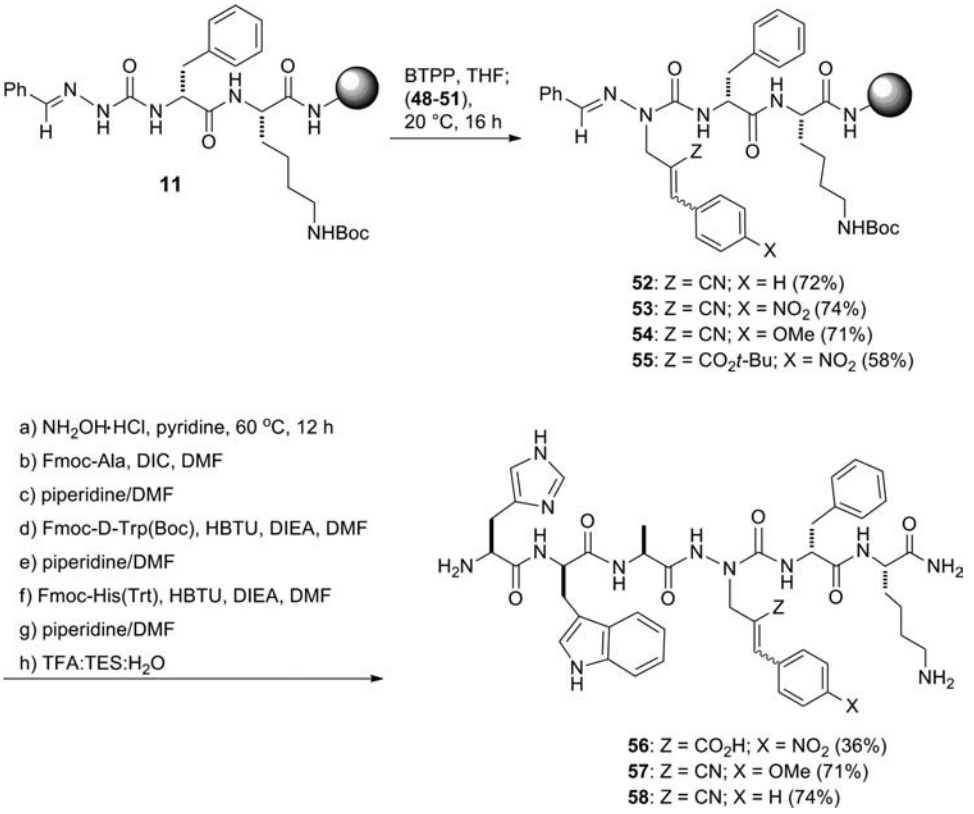

[a] Crude purities were ascertained from cleavage of resin aliquots using TFA/H_2O/TES and LCMS analysis using 0−80% MeOH/H_2O with 0.1% FA as eluant.

and converted to a product with mass corresponding to that of the aza-pyroglutamate, aza-pGlu, **59** (55%, Scheme 5).[26] Although such annulation may be avoided by amide side-chain protection,[27] aza-pyroglutamate **64** was pursued instead as a His^1 replacement in the hope of improving pharmacokinetic properties.[8]

Similarly, alkyl vinyl ketones were used to replace His^1 with aza-dehydroprolines (Scheme 6). Resin-bound aza-Gly hexapeptide **60** was treated with BTPP (300 mol %) and exposed respectively to acrylamide, as well as methyl and ethyl vinyl ketones (300 mol %), to afford alkyl semicarbazones **61**−**63** in respectable conversions (60−80%), as assessed by LCMS analysis. Semicarbazone removal with hydroxylamine was followed by intramolecular annulation, such that resin cleavage provided *N*-terminal aza-pyroglutamate **64** and pyrrazolines **65** and **66** in acceptable overall yields (8−9%) and purity (90−99%) after reverse-phase HPLC purification (Table 1, entries 1−3).

CD Spectroscopy. Circular dichroism (CD) spectroscopy was used to evaluate azapeptide conformation in water (Figure 3). The CD curve shape of the parent peptide GHRP-6 is characteristic of a random coil or disordered structure featuring a negative maximum band at 190 nm, which was similarly observed for analogues **64**-**66**, possessing *N*-terminal heterocycle modifications at His^1 (Figures 3a and b).[29] Substitution of aza-Glu analogues at the Ala^3 and Trp^4 positions of GHRP-6 caused varying effects on the CD curve shape indicative of stabilization of secondary structure about the aza-residue substitution. The CD curve of [aza-Ala^3]GHRP-6[15a] also exhibits a negative maximum band at 190 nm characteristic of a random coil conformation (Figure 3c).[15,29] However, substitution at the Ala^3 position with other aza-amino acid residues in [aza-Glu^3] GHRP-6 analogues **36**-**40** revealed CD curves which suggested averaging between random coil[29] (more predominant in **39** and

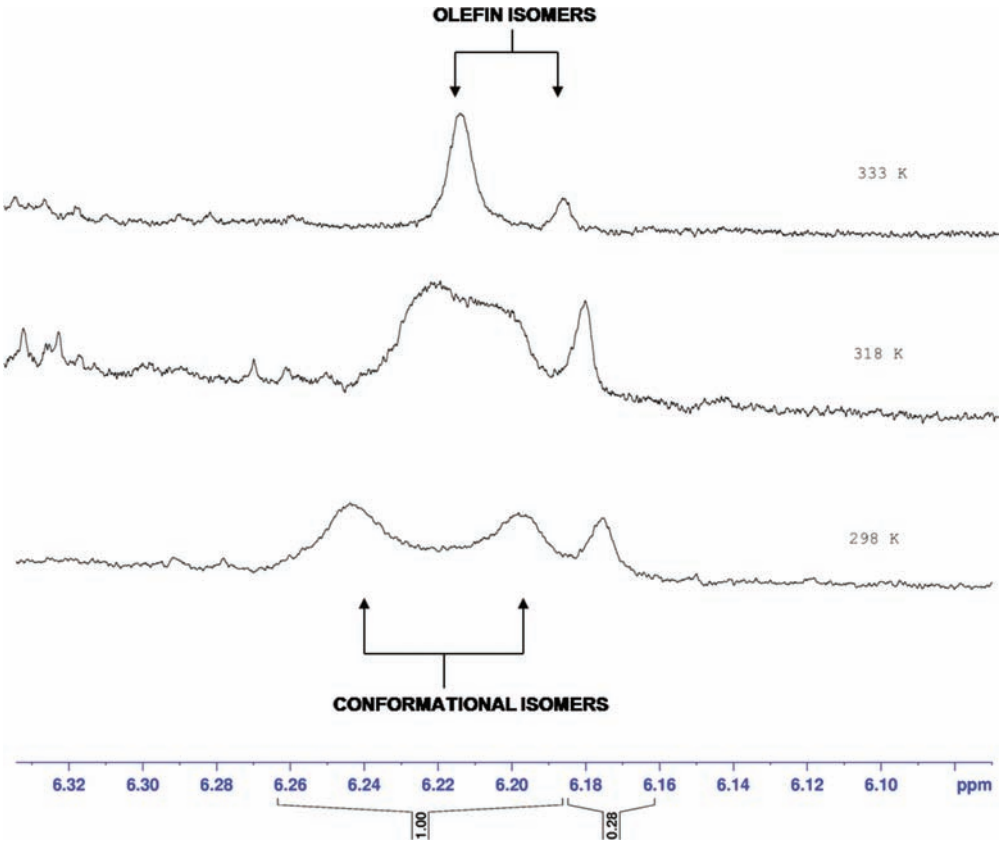

Figure 2. ^{1}H NMR spectrum of **57** at variable temperatures.

Scheme 5. Synthesis of aza-pGlu 59

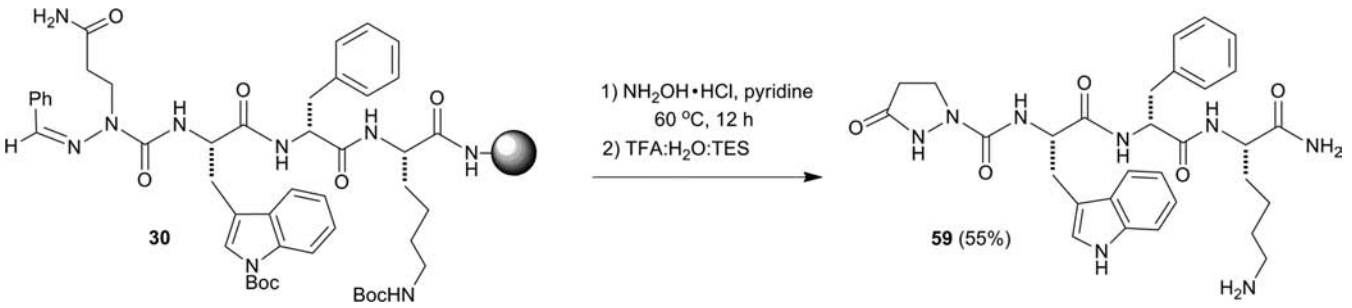

40) and polyproline type II,[31] (more predominant in **36**) or β-turn[30] (more predominant in **37** and **38**) conformations (Figure 3d). Previous studies of GHRP-6 analogues by CD spectroscopy have shown that replacement of Trp^4 by an aza-Phe^4 residue led to a conformational change in water from a curve shape characteristic of a random coil to one indicative of a β-turn (Figure 3e).[15a,28,30] The CD signatures for aza-residue modifications at Trp^4, possessing [aza-Glu^4]GHRP-6 derivatives **19**-**22**, as well as, aromatic 4-alkylidene aza-Glu^4 residues, **56**-**58**, all were indicative of β-turn conformers characterized by negative maximum around 200 and 230 nm and a positive maximum near 215 nm, albeit **19** and **21** may have significant populations of random coil (Figure 3f).[30] Therefore, aza-residue replacements at Trp^4 appear to stabilize a β-turn conformation within the D-Trp-Ala-Trp-D-Phe region of GHRP-6 with significant tolerance of side-chain diversity.

NMR Spectroscopy. A deeper study of the azapeptide conformation of [aza-Phe^4]GHRP-6 (**2**) has begun using NMR spectroscopy to add additional support for the β-turn structure observed by CD spectroscopy. Two-dimensional COSY, TOCSY and HMQC experiments were performed to facilitate chemical shift assignments of the ^{1}H and ^{13}C NMR spectra in DMSO-d_6 at 298 K (see Experimental Section and Supporting Information for details). The ^{1}H NMR spectrum of **2** in D_2O was also used to assign NH signals. Complete structural assignments have, however, been hindered by overlapping of signals and residual H_2O and DMSO solvent peaks which masked the methylene signals of the D-Phe and D-Trp residues. Nevertheless, chemical shift values of the amide protons were employed to determine intramolecular hydrogen bonding in **2**. Chemical shifts for solvent-exposed amide protons and those involved in intramolecular hydrogen bonds are respectively observed

Scheme 6. Submonomer Solid-Phase Synthesis of Aza-pyroglutamate and Pyrrazoline Azapeptides[a]

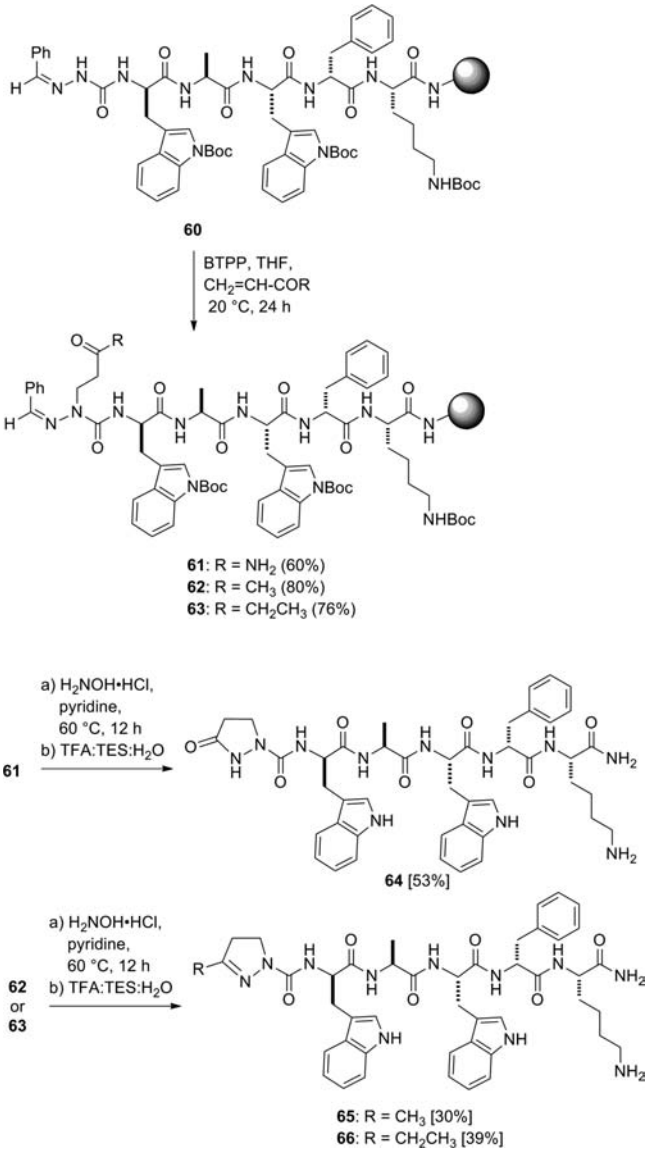

[a] Percents in parentheses refer to crude purity ascertained after resin cleavage using TFA/H_2O/TES, by LCMS analyses using 0−80% MeOH in H_2O with 0.1% FA as eluant.

between 4 and 6 ppm and between 7 and 9 ppm in model azapeptides dissolved in $CDCl_3$ at 298 K.[35] The backbone amide protons of the Ala, D-Trp, residues (8.7, and 8.2 ppm, respectively) of **2**, were shifted downfield from the remaining amide signals (7.6−7.3 ppm) in DMSO-d_6 at 298 K. The chemical shifts and temperature dependencies for the amide protons were measured in DMSO-d_6 from 283 to 383 K to distinguish H-bonding of the amide signals from those exposed to solvent. Specifically, the chemical shifts of intramolecular H-bonding amide protons show less temperature dependence ($\Delta\delta/\Delta T \leq 4$ ppb/K) than those exposed to solvent (± 6 ppb/K $\leq \Delta\delta/\Delta T \leq 10$ ppb/K).[36] In the case of azapeptide **2**, the D-Phe NH signal (7.3 ppm) exhibited a small temperature dependence ($\Delta\delta/\Delta T = -1$ ppb/K) consistent with intramolecular hydrogen bonding; on the other hand, examination of the Lys, Ala and D-Trp amide signals indicated values for solvent-exposed NHs ($\Delta\delta/\Delta T = -4$, -8, and -11 ppb/K, respectively). In the two-dimensional ROESY experiment (700 ms), a number of interactions between sequential side chain residues suggested folding about a preorganized turn conformation (see Supporting Information). The amide temperature dependencies and long-range side chain interactions were consistent with [aza-Phe^4]GHRP-6 adopting a turn geometry in which the D-Phe residue NH is engaged in an intramolecular hydrogen bond. Although the correlation of the CD and NMR spectral data for [aza-Phe^4]GHRP-6 in aqueous solution supports a β-turn, the relevance for such a conformation when **2** is bound to the receptor remains to be elucidated.

CD36 Binding. The affinities (EC_{50} values) of azapeptides containing potentially ionic side chains were evaluated in competition binding studies with the GHRP-6 prototype ligand, hexarelin (His-D-2-Me-Trp-Ala-Trp-D-Phe-Lys-NH_2, Table 2, entry 1). In this assay, [aza-Phe^4]GHRP-6 (**2**, Table 2, entry 8) exhibited slightly enhanced affinity relative to hexarelin (1.34 μM *vs.* 2.27 μM, respectively). Moreover, several [azaGlu]GHRP-6 analogues also maintained low micromolar affinity for the CD36 receptor (Table 2).

At the Ala^3 position, [aza-Ala^3]GHRP-6 (**3**) exhibited a 3-fold loss in binding affinity relative to hexarelin (6.9 μM vs 2.3 μM, Table 2, entries 1 and 2). The [aza-Glu^3]GHRP-6 analogues **36**−**38** and **40** (Table 2, entries 3−5 and 7) maintained relatively high affinity (2.4−27 μM) for the CD36 receptor. In particular, the [aza-(cyanoethyl)Gly^3]GHRP-6 analogue had affinity similar to that of hexarelin (2.4 μM vs 2.3 μM, Table 2, entries 4 and 1).

At the Trp^4 position, relative to [aza-Phe^4]GHRP-6 (**2**, 1.34×10^{-6} M), none of the novel analogues exhibited improved affinity. For example, 8- and 13-fold lower CD36 binding affinities were respectively observed for [aza-Glu^4]GHRP-6 (**19**, 11 μM) and [4-alkylidene aza-Glu^4]GHRP-6 (**56**, 18 μM) (Table 2, entries 8, 9 and 13). On the other hand, relative to the non-ionic aliphatic sequences, [azaLeu^4]GHRP-6[16a] (**67**, 2.9 mM) and [(2-cyano-*p*-methoxycinnamyl)Gly^4]GHRP-6 (**57**, 3.5 mM), [aza-Glu^4]GHRP-6 analogues **19** and **56** exhibited >150-fold higher affinity for the CD36 receptor, illustrating that the ionic carboxylate enhanced affinity relative to the simple hydrophobic aliphatic counterparts.

DISCUSSION AND CONCLUSION

Azapeptide side-chain diversity has been expanded by employing Michael acceptors and allylic acetates in conjugate addition−elimination reactions to a semicarbazone-derived aza-Gly using submonomer solid-phase azapeptide synthesis. Fifteen new aza-analogues of the GHRP-6 hexapeptide have been synthesized in acceptable isolated yields (4−13%) and purities (>90%) after HPLC purification. The phosphazene base, BTPP, proved more effective than potassium *tert*-butoxide in the Michael addition and conjugate addition−elimination reactions onto the semicarbazone. Michael adducts with reactive side chain functional groups were also found to undergo intramolecular annulation during semicarbazone deprotection to afford novel *N*-terminal pyrrazoline analogues.

Ligands of the CD36 receptor have been specifically pursued in our program to develop treatments for angiogenesis-related diseases, such as age-related macular degeneration and diabetic retinopathy, as well as atherosclerosis.[9−11] Our synthetic methodology has provided rapid access to a small library of side-chain

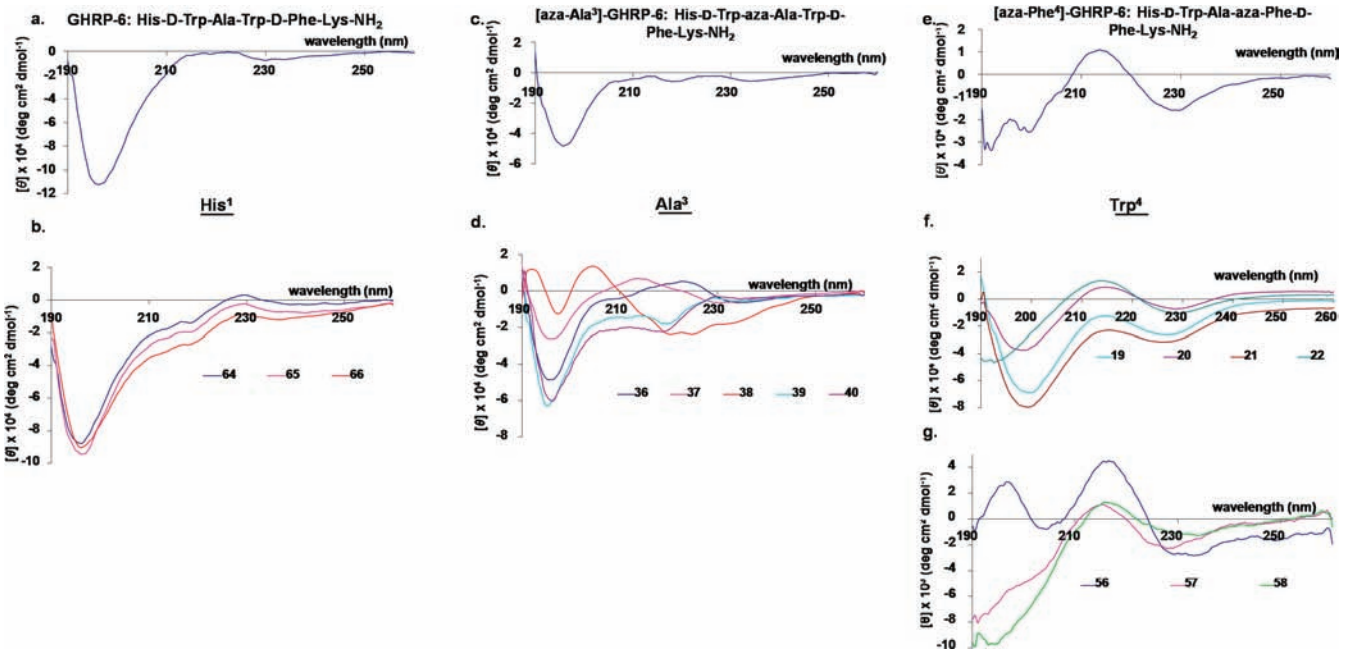

Figure 3. Circular dichroism spectra for GHRP-6 azapeptides (20 μM) in water.

Table 2. EC_{50} Binding Values for the CD36 Receptor

entry	azapeptide sequence (#)	EC_{50} binding ($\times 10^{-6}$ M)
1	His-D-2-Me-Trp-Ala-Trp-D-Phe-Lys-NH_2 (**1**)	2.27 ± 0.32
2	His-D-Trp-aza-Ala-Trp-D-Phe-Lys-NH_2 (**3**)	6.89 ± 0.21
3	His-D-Trp-aza-Glu-Trp-D-Phe-Lys-NH_2 (**36**)	26.9 ± 0.15
4	His-D-Trp-aza-(cyanoethyl)Gly-Trp-D-Phe-Lys-NH_2 (**37**)	2.36 ± 0.47
5	His-D-Trp-aza-(ethyl methylphosphoryl)Gly-Trp-D-Phe-Lys-NH_2 (**38**)	27.0 ± 0.70
6	His-D-Trp-aza-(ethyl dimethylphosphoryl)Gly-Trp-D-Phe-Lys-NH_2 (**39**)	1210 ± 1.23
7	His-D-Trp-aza-(ethyl diethylphosphoryl)Gly-Trp-D-Phe-Lys-NH_2 (**40**)	5.38 ± 0.19
8	His-D-Trp-Ala-aza-Phe-D-Phe-Lys-NH_2 (**2**)	1.34 ± 0.22
9	His-D-Trp-Ala-aza-Glu-D-Phe-Lys-NH_2 (**19**)	11.1 ± 0.20
10	His-D-Trp-Ala-aza-Leu-D-Phe-Lys-NH_2 (**67**)	2890 ± 1.56
11	His-D-Trp-Ala-aza-(ethyl methylphosphoryl)Gly-D-Phe-Lys-NH_2 (**20**)	6610 ± 1.38
12	His-D-Trp-Ala-aza-(ethyl diethylphosphoryl)Gly-D-Phe-Lys-NH_2 (**22**)	4500 ± 0.25
13	His-D-Trp-Ala-aza-(*E*/*Z*)-(2-carboxy-*p*-nitrocinnamyl)Gly-D-Phe-Lys-NH_2 (**56**)	18.4 ± 0.37
14	His-D-Trp-Ala-aza-(*E*/*Z*)-(2-cyano-*p*-methoxycinnamyl)Gly-D-Phe-Lys-NH_2 (**57**)	3530 ± 1.01

diverse GHRP-6 azapeptides for evaluating structure−activity relationships with the CD36 scavenger receptor. According to the CD spectra curve shapes, NMR and binding data, the presence of an aza-amino acid residue can influence the conformation and affinity of the GHRP-6 analogues contingent on its location in the sequence and side chain. The two aza-analogues exhibiting highest affinity possessed curve shapes indicative of β-turn geometry: [aza-(cyanoethyl)Gly^3]- and [aza-Phe^4]GHRP-6 (**37** and **2**); both had affinities (2.4 and 1.3 μM) similar to that of hexarelin (2.3 μM). Although a putative turn geometry in [aza-Phe^4]GHRP-6 was also supported by NMR spectroscopy which suggested a fold about the aza-residue, the relevance of the turn structure obtained in solution to that of the bound conformation remains to be elucidated. The loss of affinity on respective substitutions at positions 3 and 4 using the described aza-amino acid residues may be due to various factors, including incorrect backbone geometry and side-chain interactions. For example, although [aza-(ethyl methylphosphoryl)Gly^4]- and [aza-(ethyl diethylphosphoryl) Gly^4]GHRP-6 (**20** and **22**) exhibited curve shapes indicative of β-turn geometry, neither possessed significant affinity for the CD36 receptor. The aza-glutamate analogues, [aza-Glu^4]- and [aza-(*E*/*Z*)-(2-carboxy-*p*-nitrocinnamyl)Gly^4]GHRP-6 (**19** and **56**), featuring ionic side chains at the Trp^4 position, both exhibited interesting affinity (18 and 27 μM) for the CD36 receptor, >150-fold superior to their counterparts possessing aliphatic side chains: [aza-Leu^4]- and [aza-(*E*/*Z*)-(2-cyano-*p*-methoxycinnamyl)Gly^4]GHRP (**67** and **57**). The manner by which such ionic side chains improve affinity relative to aliphatic counterparts remains a matter of debate; however, their potential to form salt bridges with conserved lysine residue side chains within the CD36 receptor emerges as an interesting hypothesis

dx.doi.org/10.1021/ja203007u |*J. Am. Chem. Soc.* 2011, 133, 12493–12506

for future ligand design. In conclusion, the submonomer synthesis method offers a powerful means for making azapeptides for studying structure−activity relationships with target receptors. Employing this method, we are now studying the anti-angiogenic and anti-atherosclerotic effects of such ligands in pursuit of their full therapeutic potential.

EXPERIMENTAL SECTION

General Methods. Polystyrene Rink Amide resin (0.67 mmol/g) was purchased from Advanced Chemtech, and the manufacturer's reported loading of the resin was used in the calculation of the yields of the final products. Benzaldehyde, *p*-nitrobenzaldehyde, *p*-methoxybenzaldehyde, acetyl chloride, *tert*-butyl acrylate, acrylonitrile, phenylvinyl sulfate, diethylvinyl phosphate, dimethylvinyl phosphate, acrylamide, methylvinyl ketone, ethylvinyl ketone, hydrazine hydrate, *p*-nitrophenyl chloroformate, potassium *tert*-butoxide, *tert*-butylimino-tri(pyrrolidino) phosphorane (BTPP), hydroxylamine hydrochloride, pyridine, formic acid (FA), and *N*,*N*-diisopropylethylamine (DIEA) were all purchased from Aldrich and used without further purification. Thin-layer chromatography (TLC) was performed on silica gel 60 F254 plates from Merck. Commercially available Fmoc amino acids, Fmoc-His(Trt), Fmoc-D-Trp(Boc), Fmoc-Ala, Fmoc-Trp(Boc), Fmoc-D-Phe, and FmocLys-(Boc) and coupling reagents such as HBTU and diisopropylcarbodiimide (DIC) were purchased from GL Biochem and used as received. All solvents were obtained from VWR International. Anhydrous solvents [*N*,*N*-dimethylformamide (DMF), tetrahydrofuran (THF), and dichloromethane (DCM)] were obtained by passage through solvent filtration system (Glass-Contour, Irvine, CA).

2-[Hydroxyl(phenyl)methyl]acrylonitrile (44). A stirred solution of benzaldehyde (0.5 g, 4.7 mmol) and 25 wt % aqueous trimethylamine (1.5 mL, 5.9 mmol) in methanol (2.5 mL) was treated with acrylonitrile (0.94 mL, 14.2 mmol) dropwise over the span of 5 min at room temperature (20 °C). The clear solution was stirred until TLC indicated formation of a more polar product without further consumption of starting material [(2:1 Hexane/EtOAc), R_f (benzaldehyde): 0.7 and R_f (**44**): 0.4]. The crude was diluted in chloroform (20 mL) and treated with water (5 mL). The organic phase was separated, and the aqueous phase was extracted with chloroform (2 × 10 mL). The combined organic extracts were dried over anhydrous magnesium sulfate and evaporated in vacuo. The crude product was purified by column chromatography using 2:1 Hexane/EtOAc to afford the pure adduct (**44**) as a colorless oil. Yield (486 mg, 65%), ^{1}H NMR (400 MHz, $CDCl_3$) δ 3.14 (d, J = 4 Hz, 1H), 5.25 (d, J = 4 Hz, 1H), 6.0 (s, 1H), 6.08 (s, 1H), 7.37−7.43 (m, 5H). ^{13}C NMR (100 MHz, $CDCl_3$) δ 73.68, 116.7, 125.8, 126.2, 128.6, 129.7, 138.8. HRMS Calcd m/z for $C_{10}H_{10}NO$ $[M + H]^+$ 160.0757, found 160.0758.

2-[Hydroxyl(4-nitrophenyl)methyl]acrylonitrile (45). **45** was prepared as described for **44** above and isolated by silica gel column chromatography using 2:1 Hexane/EtOAc, R_f (2:1 Hexane/EtOAc) 0.2, pale-yellow oil. Yield (620 mg, 46%); ^{1}H NMR (400 MHz, $CDCl_3$) δ 3.60 (br., 1H), 5.44 (s, 1H), 6.09 (s, 1H), 6.19 (s, 1H), 7.59 (d, J = 12 Hz, 2H), 8.20 (t, J = 4 Hz, 2H); ^{13}C NMR (100 MHz, $CDCl_3$) δ 72.73, 116.1, 123.6, 124.9, 127.1, 131.2, 146.0, 147.5; HRMS Calcd m/z for $C_{10}H_9N_2O_3$ $[M + H]^+$ 205.0608, found 205.0613.

2-[Hydroxyl(4-methoxyphenyl)methyl]acrylonitrile (46). **46** was prepared as described for **44** above and isolated by silica gel column chromatography using 2:1 Hexane/EtOAc, R_f (2:1 Hexane/EtOAc): 0.2, colorless oil. Yield (344 mg, 25%); ^{1}H NMR (400 MHz, $CDCl_3$) δ 3.30 (d, J = 4 Hz, 1H), 3.80 (s, 3H), 5.18 (s, 1H), 5.97 (s, 1H), 6.06 (s, 1H), 6.90 (dd, J = 4, 6 Hz, 2H), 7.27 (d, J = 8 Hz, 2H); ^{13}C NMR (100 MHz, $CDCl_3$) δ 55.0, 73.2, 113.9, 114.1, 116.8, 126.1, 127.6, 128.1, 129.2, 131.1, 159.5; HRMS Calcd m/z for $C_{11}H_{12}NO_2$ $[M + H]^+$ 190.0863, found 190.0856

2-[Hydroxyl(4-nitrophenyl)methyl]-*tert*-butylacrylate (47). **47** was prepared as described for **44** above and isolated by silica gel column chromatography using 4:1 Hexane/EtOAc, R_f (2:1 Hexane/EtOAc): 0.7, pale-yellow oil. Yield (890 mg, 47%); ^{1}H NMR (400 MHz, $CDCl_3$) δ 1.43 (s, 9H) 3.53 (d, J = 8 Hz, 1H), 5.58 (d, J = 8 Hz, 1H), 5.77 (s, 1H), 6.31 (s, 1H), 7.58 (d, J = 12 Hz, 2H), 8.21 (t, J = 4 Hz, 2H); ^{13}C NMR (100 MHz, $CDCl_3$) δ 27.6, 72.6, 82.0, 123.2, 126.2, 126.9, 141.9, 147.0, 148.7, 164.9; HRMS Calcd m/z for $C_{14}H_{17}NO_5Na$ $[M + Na]^+$ 302.0999, found 302.1007.

2-[Acetyloxy(phenyl)methyl]acrylonitrile (48). A stirred solution of alcohol **44** (0.5 g, 3.2 mmol) in pyridine (0.4 mL, 4.9 mmol) and dichloromethane (3.5 mL) was treated with acetyl chloride (0.3 mL, 4.2 mmol) dropwise over 5 min at room temperature (20 °C). The clear solution was stirred until TLC indicated complete product formation [(2:1 Hexane/EtOAc) R_f (**48**): 0.5]. The crude was diluted in dichloromethane (10 mL) and washed with water (10 mL) and brine (10 mL). The organic phase was separated and dried over anhydrous magnesium sulfate, and the extracts were evaporated in vacuo. The crude product was purified by column chromatography using 2:1 Hexane/EtOAc to afford acetate **48** as a yellow oil. Yield (660 mg, 61%); ^{1}H NMR (400 MHz, $CDCl_3$) δ 2.17 (s, 3H), 6.02 (d, J = 4 Hz, 1H), 6.07 (d, J = 4 Hz, 1H), 6.35 (s, 1H), 7.39−7.42 (m, 5H). ^{13}C NMR (100 MHz, $CDCl_3$) δ 20.5, 74.0, 115.9, 122.8, 126.6, 128.6, 128.9, 131.8, 135.3, 168.9. HRMS Calcd m/z for $C_{12}H_{11}NO_2Na$ $[M + Na]^+$ 224.0682, found 224.0688.

2-[Acetyloxy(4-nitrophenyl)methyl]acrylonitrile (49). **49** was prepared as described for **48** above and isolated by silica gel column chromatography using 2:1 Hexane/EtOAc, R_f (2:1 Hexane/EtOAc) 0.5, orange oil. Yield (300 mg, 47%); ^{1}H NMR (400 MHz, $CDCl_3$) δ 2.22 (s, 3H), 6.17 (d, J = 12 Hz, 2H), 6.42 (s, 1H), 7.61 (d, J = 8 Hz, 2H), 8.26 (d, J = 8 Hz, 2H). ^{13}C NMR (100 MHz, $CDCl_3$) δ 20.5, 73.1, 115.2, 121.6, 123.8, 127.5, 133.0, 142.2, 147.9. 168.7. HRMS Calcd m/z for $C_{12}H_9N_2O_4$ $[M - H]^-$ 245.0567, found 245.057.

2-[Acetyloxy(4-methoxyphenyl)methyl]acrylonitrile (50). **50** was prepared as described for **48** above and isolated by silica gel column chromatography using 2:1 Hexane/EtOAc, R_f (2:1 Hexane/EtOAc) 0.5, yellow oil. Yield (198 mg, 64%); ^{1}H NMR (400 MHz, $CDCl_3$) δ 2.16 (s, 3H), 3.82 (s, 3H), 6.00 (s, 1H), 6.06 (s, 1H), 6.30 (s, 1H), 6.93 (t, J = 4 Hz, 2H), 7.34 (d, J = 8 Hz, 2H). ^{13}C NMR (100 MHz, $CDCl_3$) δ 20.6, 55.0, 73.7, 113.9, 116.0, 123.0, 127.3, 128.2, 131.2, 159.9, 168.9. HRMS Calcd m/z for $C_{13}H_{13}NO_3Na$ $[M + Na]^+$ 254.0788, found 254.0791.

2-[Acetyloxy(4-nitrophenyl)methyl]-*tert*-butylacrylate (51). **51** was prepared as described for **48** above and isolated by silica gel column chromatography using 2:1 Hexane/EtOAc, R_f (1:1 Hexane/EtOAc) 0.8, pale-yellow oil. Yield (876 mg, 92%); ^{1}H NMR (400 MHz, $CDCl_3$) δ 1.40 (s, 9H), 2.14 (s, 3H), 5.85 (s, 1H), 6.39 (s, 1H), 6.69 (s, 1H), 7.57 (d, J = 8 Hz, 2H), 8.21 (d, J = 8 Hz, 2H). ^{13}C NMR (100 MHz, $CDCl_3$) δ 20.60, 27.54, 71.89, 81.63, 123.2, 125.5, 128.2, 139.6, 145.0, 147.3, 163.2, 168.8. HRMS Calcd m/z for $C_{16}H_{19}NO_6Na$ $[M + Na]^+$ 344.11046, found 344.10993.

Fmoc-based SPPS: Fmoc Deprotection and Peptide Couplings. Peptide syntheses were performed under standard conditions[18] on an automated shaker using Polystyrene Rink Amide resin (0.67 mmol/g). Couplings of amino acids (3 equiv) were performed in DMF using HBTU (3 equiv) as coupling reagent and DIEA (6 equiv) for 3 h. Fmoc deprotections were performed by treating the resin with 20% piperidine in DMF for 30 min. Resin was washed after each coupling and deprotection step sequentially with DMF (3 × 10 mL), MeOH (3 × 10 mL), THF (3 × 10 mL), and DCM (3 × 10 mL). The purity of di-[D-Phe-Lys-NH_2], tri-[Trp-D-Phe-Lys-NH_2], and penta-[D-Trp-Ala-Trp-D-Phe-Lys-NH_2] peptide fragments was ascertained by LCMS analysis after cleavage and deprotection of a small aliquot of resin.

Azapeptide couplings were performed according to the symmetric anhydride method.[32] Fmoc-amino acids (10 equiv) were activated with diisopropylcarbodiimide (5 equiv) in dry DCM at 0 °C for 20 min. The suspension was concentrated in vacuo, dissolved in DMF, and added to the semicarbazide resin. The reaction was continued for 24 h at room temperature, and the resin was filtered and washed under vacuum with DMF (3 × 10 mL), MeOH (3 × 10 mL), THF (3 × 10 mL), and DCM (3 × 10 mL). The extent of reaction was monitored by subjecting an aliquot (3 mg) of resin to Fmoc deprotection (20% piperidine/DMF, 0.3 mL, 30 min) followed by the cleavage conditions [0.3 mL, TFA/TES/H_2O (95:2.5:2.5, v/v/v)], and the crude was analyzed by LCMS. The target sequences were completed according to the conventional Fmoc-based SPPS.[18]

Cleavage Test of Resin-Bound Peptide. A sample of peptide-bound resin (3−5 mg) was treated with a freshly made solution of TFA/H_2O/TES (95:2.5:2.5, v/v/v, 0.3 mL) for 30 min at room temperature. The cleavage mixture was filtered and then concentrated, and the crude peptide was precipitated with cold ether (1.5 mL). Crude peptide samples were agitated on a vortex shaker, and spun in a centrifuge. Decantation of the supernatant left a pellet, which was dissolved in 10% MeOH/H_2O (1 mg/mL) and subjected to LCMS analysis.

Representative Protocol for aza-Gly-Peptide Synthesis: Preparation of Semicarbazone-Protected aza-Gly-Peptide Resin 11. To a stirred solution of EtOH (3 mL) and hydrazine hydrate (120 μL, 3.7 mmol) at 0 °C was added benzaldehyde (190 μL, 1.9 mmol) dropwise. Complete formation of phenyl hydrazone was usually observed after 15 min by TLC, [(2:1 Hexane/EtOAc), R_f (benzaldehyde) 0.7 and R_f (benzaldehyde hydrazone) 0.6]. The mixture was poured directly into H_2O (5 mL) and extracted with DCM (3 × 5 mL). The organic phase was separated, dried with $MgSO_4$, and concentrated in vacuo to yield the benzaldehyde hydrazone as a yellow-tinged oil that was employed without further purification.

Benzaldehyde hydrazone (230 mg, 1.9 mmol, 10 equiv) in DCM (2 mL) was added dropwise over 15 min to a solution of *p*-nitrophenyl chloroformate (240 mg, 1.2 mmol, 6 equiv) in DCM (2 mL) at 0 °C. The reaction mixture was stirred at room temperature under argon for an additional 1.5 h, and treated with DIEA (420 μL, 2.4 mmol, 12 equiv) dropwise over 20 min at 0 °C, when TLC [(2:1 Hexane/EtOAc), R_f: 0.75] indicated complete conversion to the activated methylidene carbazate intermediate. The suspension was quickly transferred to the resin (250 mg, 0.19 mmol). The resin suspension was agitated on an automated shaker for 16 h at room temperature, filtered, washed under vacuum with DMF (3 × 10 mL), MeOH (3 × 10 mL), THF (3 × 10 mL), and DCM (3 × 10 mL). The extent of reaction conversion was monitored on an aliquot (3 mg) of resin which was subjected to 0.3 mL of TFA/TES/H_2O (95:2.5:2.5, v/v/v) for resin cleavage and the crude was analyzed by LCMS.

Benzaldehyde semicarbazone-D-Phe-Lys-NH_2 (11): LCMS (0−80% MeOH, with 0.1% FA, 10 min) R.T. = 5.9 min; LCMS (ESI) calcd for $C_{23}H_{32}N_6O_3$ $[M + 2H]^+$, 440.5 found *m/e* 441.3.

Benzaldehyde semicarbazone-Trp-D-Phe-Lys-NH_2 (24): LCMS (0−80% MeOH, with 0.1% FA, 10 min) R.T. = 6.1 min; LCMS (ESI) calcd for $C_{34}H_{42}N_8O_4$ $[M + 2H]^+$, 627.1 found *m/e* 627.3.

Benzaldehyde semicarbazone-D-Trp-Ala-Trp-D-Phe-Lys-NH_2 (60): LCMS (0−80% MeOH, with 0.1% FA, 10 min) R.T. = 6.2 min; LCMS (ESI) calcd for $C_{48}H_{57}N_{11}O_6$ $[M + 2H]^+$, 884.1 found *m/e* 884.4.

Representative Alkylation of aza-Gly, Preparation of Resin (12−14 and 52−55). To the swollen semicarbazone peptide bound resin **11** (0.05 g, 33 μmol) in THF (1 mL), potassium *tert*-butoxide (12 mg, 0.1 mmol, 3 equiv) or BTPP (30 μL, 0.1 mmol, 3 equiv) was added followed by Michael acceptor or allylic acetate (**48**−**51**) (0.1 mmol, 3 equiv). After agitation at room temperature for 16 h, the resin was filtered, washed with DMF (2 × 10 mL), MeOH (2 × 10 mL), THF (2 × 10 mL), and DCM (2 × 10 mL) and dried under vacuum. The extent of reaction conversion was monitored on an aliquot (3 mg) of resin which was subjected to 0.3 mL of TFA/TES/H_2O (95:2.5:2.5, v/v/v) for resin cleavage, and the crude was analyzed by LCMS.

Benzaldehyde semicarbazone-(glutamyl)-D-Phe-Lys-NH_2 (12): LCMS (0−80% MeOH, with 0.1% FA, 10 min) R.T. = 5.8 min; LCMS (ESI) calcd for $C_{26}H_{36}N_6O_5$ $[M + 2H]^+$, 513.0 found *m/e* 513.2.

Benzaldehyde semicarbazone-(ethyl dimethylphosphate)-D-Phe-Lys-NH_2 (13): LCMS (0−80% MeOH, with 0.1% FA, 10 min) R.T. = 5.8 min; LCMS (ESI) calcd for $C_{27}H_{41}N_6O_6P$ $[M + 2H]^+$, 577.0 found *m/e* 577.2.

Benzaldehyde semicarbazone-(ethyl diethylphosphate)-D-Phe-Lys-NH_2 (14): LCMS (0−80% MeOH, with 0.1% FA, 10 min) R.T. = 5.9 min; LCMS (ESI) calcd for $C_{29}H_{45}N_6O_6P$ $[M + 2H]^+$, 605.0 found *m/e* 605.2.

Benzaldehyde semicarbazone-(*E/Z*)-(2-cyanocinnamyl)-D-Phe-Lys-NH_2 (52): LCMS (0−80% MeOH, with 0.1% FA, 10 min) R.T. = 6.2 min; LCMS (ESI) calcd for $C_{33}H_{39}N_7O_3$ $[M + 2H]^+$, 581.7 found *m/e* 582.3.

Benzaldehyde semicarbazone-(*E/Z*)-(2-cyano-*p*-nitrocinnamyl)-D-Phe-Lys-NH_2 (53): LCMS (0−80% MeOH, with 0.1% FA, 10 min) R.T. = 6.3 min; LCMS (ESI) calcd for $C_{33}H_{38}N_8O_5$ $[M + 2H]^+$, 626.7 found *m/e* 627.3.

Benzaldehyde semicarbazone-(*E/Z*)-(2-cyano-*p*-methoxycinnamyl)-D-Phe-Lys-NH_2 (54): LCMS (0−80% MeOH, with 0.1% FA, 10 min) R.T. = 6.3 min; LCMS (ESI) calcd for $C_{34}H_{41}N_7O_4$ $[M + 2H]^+$, 611.7 found *m/e* 612.2.

Benzaldehyde semicarbazone-(*E/Z*)-(2-carboxy-*p*-nitrocinnamyl)-D-Phe-Lys-NH_2 (55): LCMS (0−80% MeOH, with 0.1% FA, 10 min) R.T. = 6.4 min; LCMS (ESI) calcd for $C_{33}H_{39}N_7O_7$ $[M + 2H]^+$, 645.7 found *m/e* 646.2.

Benzaldehyde semicarbazone-(glutamyl)-Trp-D-Phe-Lys-NH_2 (25): LCMS (0−80% MeOH, with 0.1% FA, 10 min) R.T. = 6.5 min; LCMS (ESI) calcd for $C_{37}H_{46}N_8O_6$ $[M + 2H]^+$, 698.8 found *m/e* 699.3.

Benzaldehyde semicarbazone-(cyanoethyl)-Trp-D-Phe-Lys-NH_2 (26): LCMS (0−80% MeOH, with 0.1% FA, 10 min) R.T. = 5.4 min; LCMS (ESI) calcd for $C_{37}H_{45}N_9O_4$ $[M + 2H]^+$, 679.8 found *m/e* 680.3.

Benzaldehyde semicarbazone-(ethyl dimethylphosphate)-Trp-D-Phe-Lys-NH_2 (27): LCMS (0−80% MeOH, with 0.1% FA, 10 min) R.T. = 6.2 min; LCMS (ESI) calcd for $C_{38}H_{51}N_8O_7P$ $[M + 2H]^+$, 762.8 found *m/e* 763.2.

Benzaldehyde semicarbazone-(ethyl diethylphosphate)-Trp-D-Phe-Lys-NH_2 (28): LCMS (0−80% MeOH, with 0.1% FA, 10 min) R.T. = 6.7 min; LCMS (ESI) calcd for $C_{40}H_{55}N_8O_7P$ $[M + 2H]^+$, 790.9 found *m/e* 791.3.

Benzaldehyde semicarbazone-(ethylphenylsulfonyl)-Trp-D-Phe-Lys-NH_2 (29): LCMS (0−80% MeOH, with 0.1% FA, 10 min) R.T. = 6.3 min; LCMS (ESI) calcd for $C_{42}H_{50}N_8O_6S$ $[M + 2H]^+$, 794.9 found *m/e* 795.3.

Benzaldehyde semicarbazone-(glutaminyl)-Trp-D-Phe-Lys-NH_2 (30): LCMS (0−80% MeOH, with 0.1% FA, 10 min) R.T. = 6.2 min; LCMS (ESI) calcd for $C_{37}H_{47}N_9O_5$ $[M + 2H]^+$, 697.8 found *m/e* 698.3.

Benzaldehyde semicarbazone-(glutaminyl)-D-Trp-Ala-Trp-D-Phe-Lys-NH_2 (61): LCMS (0−80% MeOH, with 0.1% FA, 20 min) R.T. = 14.5 min; LCMS (ESI) calcd for $C_{51}H_{62}N_{12}O_7$ $[M + 2H]^+$, 955.1 found *m/e* 955.3.

Benzaldehyde semicarbazone-(ethyl methylketone)-D-Trp-Ala-Trp-D-Phe-Lys-NH_2 (62): LCMS (0−80% MeOH, with 0.1% FA, 10 min) R.T. = 6.5 min; LCMS (ESI) calcd for $C_{52}H_{63}N_{11}O_7$ $[M + 2H]^+$, 954.1 found *m/e* 954.4.

Benzaldehyde semicarbazone-(ethyl ethylketone)-D-Trp-Ala-Trp-D-Phe-Lys-NH_2 (63): LCMS (0−80% MeOH, with 0.1% FA, 10 min) R.T. = 6.5 min; LCMS (ESI) calcd for $C_{53}H_{65}N_{11}O_7$ $[M + 2H]^+$, 968.1 found *m/e* 968.4.

Representative Protocol for Semicarbazone Removal, Preparation of Aza-pGlu-Trp-D-Phe-Lys-Peptide Resin 59. Resin-bound semicarbazone **30** (0.05 g, 33 μmol) was treated with a solution of 1.5 M $NH_2OH \cdot HCl$ in pyridine (2.5 mL) and heated with ultrasound at 60 °C for 12 h. The resin was filtered and washed under vacuum with 10% DIEA/DMF (3 × 10 mL), DMF (3 × 10 mL), MeOH (3 × 10 mL), THF (3 × 10 mL), and DCM (3 × 10 mL). The extent of reaction conversion was monitored on an aliquot (3 mg) of resin, which was subjected to 0.3 mL of TFA/TES/H_2O (95:2.5:2.5, v/v/v) for resin cleavage, and the crude was analyzed by LCMS.

Aza-pGlu-Trp-D-Phe-Lys-peptide resin 59: LCMS (0−80% MeOH, with 0.1% FA, 10 min) R.T. = 5.7 min; LCMS (ESI) calcd for $C_{30}H_{38}N_8O_5$ $[M]^+$, 590.7 found *m/e* 591.2.

Deprotection and Cleavage of Azapeptide from the Resin. The Rink resin-bound peptide was deprotected and cleaved from the support using a freshly made solution of TFA/H_2O/TES (95:2.5:2.5, v/v/v, 20 mL/g of peptide resin) at room temperature for 2 h. The resin was filtered and rinsed with 1 mL of TFA. The filtrate and rinses were concentrated under a flow of $Ar_{(g)}$ until a crude oil persisted, from which a precipitate was obtained by addition of cold ether (10−15 mL). After centrifugation (12 000 rpm for 10 min.), the supernatant was removed, and the crude peptide was taken up in aqueous methanol (10% v/v) and freeze-dried to a white solid prior to analysis.

Analysis and Purification of Azapeptides. Analyses and characterization of crude azapeptides were performed on either an Agilent Technologies 1100 series LCMS instrument with ESI ion-source, single quadropole mass detection and positive mode ionization or a ThermoFinnigan LCQ Advantage MS with ESI ion-source, ion-trap mass detection, positive mode ionization and equipped with a Gilson LC 322 pump containing autosampler and injector. Azapeptide samples were dissolved in 10% H_2O in methanol. The LCMS analyses were performed on a Gemini C_{18} reverse-phase column (150 mm × 4.60 mm, 5 μm), using binary solvent system consisting of 0.1% formic acid in H_2O, and 0.1% formic acid in methanol at a flow rate of 0.5 mL/min and UV detection at 214 nm. Linear gradients of the mobile phase (0.1% formic acid in methanol, 0−80% over 15 min) were used for analyses of crude peptides.

Purification of peptides was conducted on a Waters PrepLC instrument equipped with a reverse-phase Gemini C_{18} column (250 mm × 21.2 mm, 5 μm), using binary solvent system consisting of 0.1% formic acid in H_2O, and 0.1% formic acid in methanol at a flow rate of 10 mL/min and UV detection at 214 nm. Linear gradients of the mobile phase (0.1% formic acid in methanol, 0−80% in 20 min) were used for purifications of peptides. Fractions containing pure azapeptide were combined, freeze-dried and lyophilized to a white powder. Purified azapeptide samples were analyzed for purity by LCMS with a Gemini C_{18} reverse-phase column (150 × 4.60 mm, 5 μm), with a flow rate of 0.5 mL/min using a 0−80% gradient from water (0.1% FA) to CH_3CN (0.1% FA) or to MeOH (0.1% FA).

His-D-Trp-Ala-azaPhe-D-Phe-Lys-NH_2 (2): Yield (1.2 mg, 5%), ^{1}H NMR (700 MHz, DMSO-d_6) δ 1.11 (5H, d, J = 7.49 Hz), 1.44 (3H, br s), 1.67 (1H, br s), 2.51−2.52 (1H, m), 2.69−2.71 (3H, m), 2.77 (1H, dd, J = 4.8 10 Hz), 2.96−3.01 (3H, m), 3.11−3.19 (1H, m), 3.52−3.54 (1H, m), 3.99 (1H, m), 4.06 (1H, br s), 4.30 (1H, m), 4.62 (1H, br s), 6.79 (1H, s), 6.94 (1H, t, J = 15 Hz), 7.05 (1H, t, J = 15 Hz), 7.11 (2H, s), 7.17−7.36 (12H, m), 7.42 (1H, s), 7.53 (1H, d, J = 8.1 Hz), 7.57 (1H, s), 8.23 (1H, s), 8.38 (1H, s), 8.72 (1H, s), 10.8 (1H, s). ^{13}C NMR (125 MHz, DMSO-d_6) δ 174.2, 173.8, 172.6, 172.2, 164.5, 158.2, 157.6, 137.7, 136.4, 135.5, 129.7, 128.8, 128.7, 128.1, 127.8, 127.6, 126.7, 124.1, 121.3, 118.8, 118.6, 111.7, 110.1, 54.9, 53.6, 52.6, 51.5, 40.3, 32.1, 31.1, 28.2, 27.1, 22.6, 17.1. LCMS (0−40% MeOH, 20 min) R.T. = 16.3 min; (0−40% MeCN, 20 min) R.T. = 13.3 min; LCMS (ESI) calcd for $C_{43}H_{55}N_{12}O_6$ $[M + H]^+$, 835.4 found *m/z* 835.2; HRMS Calcd *m/z* for $C_{43}H_{55}N_{12}O_6$ $[M + H]^+$ 835.4362, found 835.43494.

His-D-Trp-Ala-aza-Glu-D-Phe-Lys-NH_2 (19): Yield (1.4 mg, 6%), LCMS (0−80% MeOH, 20 min) R.T. = 9.56 min; (0−80% MeCN, 20 min) R.T. = 8.60 min; LCMS (ESI) calcd for $C_{39}H_{51}N_{12}O_8$ $[M + H]^+$, 816.0 found *m/z* 816.4; HRMS Calcd *m/z* for $C_{39}H_{50}N_{12}O_8$ $[M + H]^+$ 815.3947, found 815.3947.

His-D-Trp-Ala-aza-(ethyl methylphosphoryl)Gly-D-Phe-Lys-NH_2 (20): Yield (1 mg, 5%), LCMS (0−80% MeOH, 20 min) R.T. = 11.5 min; (0−80% MeCN, 20 min) R.T. = 9.46 min; LCMS (ESI) calcd for $C_{39}H_{56}N_{12}O_9P$ $[M + 2H]^+$, 868.1 found *m/z* 868.2; HRMS Calcd *m/z* for $C_{39}H_{56}N_{12}O_9P$ $[M + H]^+$ 867.4025, found 867.4016.

His-D-Trp-Ala-aza-(ethyl dimethylphosphoryl)Gly-D-Phe-Lys-NH_2 (21): Yield (0.4 mg, 4%), LCMS (0−80% MeOH, 20 min) R.T. = 9.58 min; (0−80% MeCN, 20 min) R.T. = 8.65 min; LCMS (ESI) calcd for $C_{40}H_{58}N_{12}O_9P$ $[M + H]^+$, 881.1 found *m/z* 881.4; HRMS Calcd *m/z* for $C_{40}H_{58}N_{12}O_9PNa$ $[M + H]^+$ 881.4181, found 881.4180.

His-D-Trp-Ala-aza-(ethyl diethylphosphoryl)Gly-D-Phe-Lys-NH_2 (22): Yield (1 mg, 5%), LCMS (0−80% MeOH, 20 min) R.T. = 10.9 min; (0−80% MeCN, 20 min) R.T. = 9.12 min; LCMS (ESI) calcd for $C_{42}H_{62}N_{12}O_9P$ $[M + H]^+$, 909.0 found *m/z* 909.4; HRMS Calcd *m/z* for $C_{42}H_{62}N_{12}O_9P$ $[M + H]^+$ 909.4494, found 909.4484.

His-D-Trp-Ala-aza-(*E/Z*)-(2-carboxy-*p*-nitrocinnamyl)Gly-D-Phe-Lys-NH_2 (56): Yield (1.5 mg, 9%), LCMS (0−80% MeOH, 20 min) R.T. = 14.3 min; (0−80% MeCN, 20 min) R.T. = 10.3 min; LCMS (ESI) calcd for $C_{46}H_{56}N_{13}O_{10}$ $[M + H]^+$, 950.0 found *m/z* 950.2; HRMS Calcd *m/z* for $C_{46}H_{56}N_{13}O_{10}$ $[M + H]^+$ 950.4268, found 950.4302.

His-D-Trp-Ala-aza-(*E/Z*)-(2-cyano-*p*-methoxycinnamyl)-Gly-D-Phe-Lys-NH_2 (57): Yield (1.7 mg, 12%), ^{1}H NMR (700 MHz, D_2O, T = 318 K) δ 1.08 (d, J = 4 Hz, 0.65H), 1.10 (m, 2H), 1.16 (d, J = 7 Hz, 3H), 1.61 (m, 3.6H), 1.79 (m, 2H), 2.81 (d, J = 7 Hz, 2H), 2.90 (td, J = 2, 7 Hz, 0.70H), 2.98 (td, J = 2, 7 Hz, 2H), 3.15 (d, J = 7.7 Hz, 2H), 3.84 (bs, 1H), 3.88 (s, 3H), 3.89 (s, 0.85H), 3.91 (bs, 1H), 4.13 (q, J = 7 Hz, 1H), 4.18 (dd, J = 5, 10 Hz, 1H), 4.30 (t, J = 7 Hz, 1H), 4.33 (d, J = 15 Hz, 1H), 4.48 (d, J = 15 Hz, 1H), 4.54 (t, J = 7.7 Hz 1H), 6.68 (s, 1H), 7.08 (d, J = 5.6 Hz, 2H), 7.22 (bs, 2H), 7.27 (bs, 2H), 7.31 (d, J = 5 Hz, 2H), 7.33 (d, J = 7.7 Hz, 3H), 7.56 (d, J = 8.4 Hz, 1H), 7.62 (d, J = 7.7 Hz, 1H), 7.63 (d, J = 7.7 Hz, 1H), 7.79 (d, J = 9 Hz, 2H) . ^{13}C NMR (125 MHz, D_2O) δ 15.58 (16.04), 22.02 (22.24), 26.27 (26.41), 27.12 (27.33), 30.21, 30.74 (31.14), 37.22, 39.21 (39.27), 40.52, 49.25 (50.27), 51.99, 53.41, 53.68, 54.20, 54.75, 54.88, 55.65, 56.61, 102.2, 108.9, 112.0, 114.4, 114.6 (114.5), 118.4, 119.3 (119.4), 122.1, 124.5, 126.0, 126.9, 127.3, 128.8 (128.9), 129.4, 130.4, 130.9 (131.0), 135.9, 136.3 (136.5), 148.3, 157.6, 161.2, 171.1, 174.2, 174.4, 175.7, 176.6. LCMS (0−80% MeOH, 20 min) R.T. = 11.8 min; (0−80% MeCN, 20 min) R.T. = 9.33 min; LCMS (ESI) calcd for $C_{47}H_{58}N_{13}O_7$ $[M + H]^+$, 916.0 found *m/z* 916.4; HRMS Calcd *m/z* for $C_{44}H_{58}N_{13}O_7$ $[M + H]^+$ 916.4577, found 916.4601.

His-D-Trp-Ala-aza-(*E/Z*)-(2-cyano-cinnamyl)Gly-D-Phe-Lys-NH_2 (58): Yield (1.6 mg, 13%), LCMS (0−80% MeOH, 20 min) R.T. = 11.4 min; (0−80% MeCN, 20 min) R.T. = 9.20 min; LCMS (ESI) calcd for $C_{44}H_{56}N_{13}O_6$ $[M + H]^+$, 886.0 found *m/z* 886.4; HRMS Calcd *m/z* for $C_{46}H_{56}N_{13}O_6$ $[M + H]^+$ 886.4471, found 886.44845.

His-D-Trp-aza-Glu-Trp-D-Phe-Lys-NH_2 (36): Yield (2.7 mg, 10%), LCMS (0−80% MeOH, 20 min) R.T. = 11.3 min; (0−80% MeCN, 20 min) R.T. = 8.96 min; LCMS (ESI) calcd for $C_{47}H_{58}N_{13}O_8$ $[M + H]^+$, 932.0 found *m/z* 932.4; HRMS Calcd *m/z* for $C_{47}H_{58}N_{13}O_8$ $[M + H]^+$ 932.4526, found 932.4542.

His-D-Trp-aza-(cyanoethyl)Gly-Trp-D-Phe-Lys-NH_2 (37): Yield (1.2 mg, 5%), LCMS (0−80% MeOH, 20 min) R.T. = 10.7 min; (0−80% MeCN, 20 min) R.T. = 8.85 min; LCMS (ESI) calcd for $C_{47}H_{57}N_{14}O_6$ $[M + H]^+$, 913.0 found m/z 913.4; HRMS Calcd m/z for $C_{47}H_{57}N_{14}O_6$ $[M + H]^+$ 913.4580, found 913.4573.

His-D-Trp-aza-(ethyl methylphosphoryl)Gly-Trp-D-Phe-Lys-NH_2 (38): Yield (1 mg, 6%), LCMS (0−80% MeOH, 20 min) R.T. = 13.7 min; (0−80% MeCN, 20 min) R.T. = 10.1 min; LCMS (ESI) calcd for $C_{47}H_{61}N_{13}O_9P$ $[M + H]^+$, 982.1 found m/z 982.4; HRMS Calcd m/z for $C_{47}H_{61}N_{13}O_9P$ $[M + H]^+$ 982.4447, found 982.4455.

His-D-Trp-aza-(ethyl dimethylphosphoryl)Gly-Trp-D-Phe-Lys-NH_2 (39): Yield (1.2 mg, 4%), LCMS (0−80% MeOH, 20 min) R.T. = 11.2 min; (0−80% MeCN, 20 min) R.T. = 8.71 min; LCMS (ESI) calcd for $C_{48}H_{63}N_{13}O_9P$ $[M + H]^+$, 997.1 found m/z 997.4; HRMS Calcd m/z for $C_{50}H_{62}N_{13}O_9PNa$ $[M + Na]^+$ 1018.4423, found 1018.4407.

His-D-Trp-aza-(ethyl diethylphosphoryl)Gly-Trp-D-Phe-Lys-NH_2 (40): Yield (1 mg, 4%), LCMS (0−80% MeOH, 20 min) R.T. = 12.2 min; (0−80% MeCN, 20 min) R.T. = 9.31 min; LCMS (ESI) calcd for $C_{50}H_{67}N_{13}O_9P$ $[M + H]^+$, 1024.1 found m/z 1024.4; HRMS Calcd m/z for $C_{50}H_{67}N_{13}O_9P$ $[M + H]^+$ 1024.4917, found 1024.4918.

aza-pGlu-D-Trp-Ala-Trp-D-Phe-Lys-NH_2 (64): Yield (2.0 mg, 9%), LCMS (0−80% MeOH, 20 min) R.T. = 16.7 min; (0−80% MeCN, 20 min) R.T. = 12.0 min; LCMS (ESI) calcd for $C_{44}H_{54}N_{11}O_7$ $[M + H]^+$, 848.0 found m/z 848.4; HRMS Calcd m/z for $C_{44}H_{54}N_{11}O_7$ $[M + H]^+$ 848.4202, found 848.4209.

2-Methyl-pyrrazoline-D-Trp-Ala-Trp-D-Phe-Lys-NH_2 (65): Yield (2.6 mg, 8%), LCMS (0−80% MeOH, 20 min) R.T. = 18.8 min; (0−80% MeCN, 20 min) R.T. = 14.0 min; LCMS (ESI) calcd for $C_{45}H_{56}N_{11}O_6$ $[M + H]^+$, 846.0 found m/z 846.4; HRMS Calcd m/z for $C_{45}H_{56}N_{11}O_6$ $[M + H]^+$ 846.4410, found 846.4417.

2-Ethyl-pyrrazoline-D-Trp-Ala-Trp-D-Phe-Lys-NH_2 (66): Yield (2.8 mg, 8%), LCMS (0−80% MeOH, 20 min) R.T. = 19.4 min; (0−80% MeCN, 20 min) R.T. = 14.4 min; LCMS (ESI) calcd for $C_{46}H_{58}N_{11}O_6$ $[M + H]^+$, 860.0 found m/z 860.4; HRMS Calcd m/z for $C_{46}H_{58}N_{11}O_6$ $[M + H]^+$ 860.4566, found 860.4566.

Mass Spectrometry. Accurate mass measurements were performed on a LC-MSD-TOF instrument from Agilent technologies in positive electrospray mode. Either protonated molecular ions $[M + H]^+$ or sodium adducts $[M + Na]^+$ were used for empirical formula confirmation.

CD Spectroscopy. All CD spectra were recorded on a Chirascan CD Spectrometer (Applied Photophysics, Leatherhead, United Kingdom) using a 1.0 cm path length quartz cell containing 20 μM of peptide dissolved in Milli-Q water. The experimental settings were: 1 nm, bandwidth; 0.5 nm, step size; 3 s, sampling time.

NMR Spectroscopy. ^1H and ^{13}C NMR spectra were measured on a Bruker NMR spectrometer (400 or 700 MHz) with samples (2−5 mM) dissolved in $CDCl_3$, DMSO-d_6 and D_2O (99.9%) and referenced to H_2O (4.79 ppm), DMSO (2.5 and 39.5 ppm) or $CHCl_3$ (7.26 and 77.8 ppm). Coupling constants, J values were measured in hertz (Hz) and chemical shift values in parts per million (ppm). For variable-temperature experiments, the sample was allowed to equilibrate within the probe, 5−10 min before the data were collected over a temperature range of 283−338 K. Two-dimensional COSY, HMQC, TOCSY (80 ms mixing time), NOESY and ROESY (150, 300, 500, and 700 ms mixing time) spectra were acquired at 298 K.

Membrane Preparation for CD36. Animal use was in accordance with the Institutional Animal Ethics Committee and the Canadian Council on Animal Care guidelines for the use of experimental animals. Sprague−Dawley (275−350 g) rats were anaesthetized with sodium pentobarbital, and their hearts were promptly removed in ice-cold saline, and the cardiac membranes were prepared according to Harigaya and Schwartz.[33]

Competitive Covalent CD36 Binding Assay Using Photoactivatable [^{125}I]-Tyr-Bpa-Ala-Hexarelin as Radioligand. The radioiodination procedure of the photoactivatable ligand and the receptor binding assays were performed as previously described by Ong et al.[34] Briefly, the rat cardiac membranes (200 μg) as source of CD36 were incubated in the darkness, in 525 μL of 50 mM Tris-HCl pH 7.4 containing 2 mM EGTA (Buffer A) in the presence of a fixed concentration of [^{125}I]-Tyr-Bpa-Ala-Hexarelin (750 000 cpm) in Buffer B (50 mM Tris-HCl pH 7.4 containing 2 mM EGTA and 0.05% Bacitracin) and of increasing concentrations of competitive ligands (ranging from 0.1 to 50 μM). Nonspecific binding was defined as binding not displaced by 50 μM peptide. After an incubation period of 60 min at 22 °C, membranes were submitted to UV irradiation with UV at 365 nm for 15 min at 4 °C. After centrifugation at 12 000 rpm for 15 min, the pellets were resuspended in 100 μL of sample buffer consisting of 62 mM Tris-HCl, pH 6.8, 2% SDS, 10% glycerol, 15% 2-mercapto-ethanol, and 0.05% bromophenol blue and boiled for 5 min prior to electrophoresis on 7.5% SDS-PAGE. The SDS/PAGE gels were fixed, colored in Coomassie Brilliant Blue R-250, dried, exposed to a storage phosphor intensifying screen (Amersham Biosciences), and analyzed by using a Typhoon PhosphorImager (Amersham Biosciences) and ImageQuant 5.0 software to establish competition curves. Protein bands corresponding to the specifically labeled protein of 87 kDa were quantified by densitometry analysis.

■ ASSOCIATED CONTENT

Supporting Information. Experimental details including analytical data, NMR spectra, LCMS chromatograms, competitive covalent binding curves for CD36 receptor binding affinities (EC_{50}). This material is available free of charge via the Internet at http://pubs.acs.org.

■ AUTHOR INFORMATION

Corresponding Author
huy.ong@umontreal.ca; william.lubell@umontreal.ca

■ ACKNOWLEDGMENT

Financial Support from the Natural Sciences and Engineering Research Council (NSERC) of Canada, le Fond Québécois de la Recherche sur la Nature et les Technologies (FQRNT) and the CIHR Team Grant Program (Funding No: CTP79848) in G-Protein Coupled Receptor Allosteric Regulation (CTIGAR) is gratefully acknowledged. We thank Dr. Alexandra Fürtös and Marie-Christine Tang for assistance in LCMS and HRMS analyses. We also thank Dr. Minh Tan Phan Viet, Cedric Malveau and Sylvie Bilodeau for assistance with NMR analyses of azapeptides **2** and **57**.

■ REFERENCES

(1) (a) Brauner-Osborne, H.; Egebjerg, J.; Nielsen, E. O.; Madsen, U.; Krogsgaard-Larsen, P. *J. Med. Chem.* **2000**, *43*, 2609–2645. (b) Stefanic, P.; Dolenc, M. S. *Curr. Med. Chem.* **2004**, *11*, 945–968.

(2) (a) Shapiro, D. A.; Kristiansen, K.; Weiner, D. M.; Kroeze, W. K.; Roth, B. L. *J. Biol. Chem.* **2002**, *277*, 11441–11449. (b) Ballesteros, J. A.; Jensen, A. D.; Liapakis, G.; Rasmussen, S. G. F.; Shi, L.; Gether, U.; Javitch, J. A. *J. Biol. Chem.* **2001**, *276*, 29171–29177.

(3) Mamonova, T.; Speranskiy, K.; Kurnikova, M. *Proteins* **2008**, *73*, 656–671.

(4) (a) Venkatraman, S.; Kong, J.-S.; Wang, Q. M.; Aube, J.; Hanzlik, R. P. *Bioorg. Med. Chem. Lett.* **1999**, *9*, 577–580. (b) Huang, Y.; Malcolm,

B. A.; Vederas, J. C. *Bioorg. Med. Chem.* **1999**, *7*, 607–619. (c) Hart, M.; Beeson, C. *J. Med. Chem.* **2001**, *44*, 3700–3709.

(5) (a) Lee, H. J.; Park, H. M.; Lee, K. B. *Biophys. Chem.* **2007**, *125*, 117–126. (b) Hammerlin, C.; Cung, M. T.; Boussard, G. *Tetrahedron Lett.* **2001**, *42*, 5009–5012. (c) Andre, F.; Boussard, G.; Marraud, M.; Didierjean, C.; Aubry, A. *Tetrahedron Lett.* **1996**, *37*, 183–186. (d) Benatalah, Z.; Aubry, A.; Boussard, G.; Marraud, M. *Int. J. Pept. Protein Res.* **1991**, *38*, 603–605.

(6) (a) Gante, J. *Synthesis* **1989**, 405–413. (b) Zega, A. *Curr. Med. Chem.* **2005**, *12*, 589–597. (c) Reviewed in: Proulx, C.; Sabatino, D.; Hopewell, R.; Spiegel, J.; Garcia Ramos, Y.; Lubell, W. D. *Future Med. Chem.* **2011**, *3*, 1139–1164.

(7) (a) Ovat, A.; Muindi, F.; Fagan, C.; Brouner, M.; Hansell, E.; Dvorak, J.; Sojka, D.; Kopacek, P.; McKerrow, J. H.; Caffrey, C. R.; Powers, J. C. *J. Med. Chem.* **2009**, *52*, 7192–7210. (b) Kato, D.; Verhelst, S. H. L.; Sexton, K. B.; Bogyo, M. *Org. Lett.* **2005**, *7*, 5649–5652.

(8) (a) Dutta, A. S.; Furr, B. J. A.; Giles, M. B.; Valcaccia, B. *J. Med. Chem.* **1978**, *21*, 1018–1024. (b) Kaur, N.; Monga, V.; Lu, X.; Gershengorn, M. C.; Jain, R. *Bioorg. Med. Chem.* **2007**, *15*, 433–443.

(9) (a) Endemann, G.; Stanton, L. W.; Madden, K. S.; Bryant, C. M.; White, R. T.; Protter, A. A. *J. Biol. Chem.* **1993**, *268*, 11811–11816. (b) Febbraio, M.; Hajjar, D. P.; Silverstein, R. L. *J. Clin. Invest.* **2001**, *108*, 785–791. (c) Avallone, R.; Demers, A.; Rodrigue-Way, A.; Bujold, K.; Harb, D.; Anghel, S.; Wahli, W.; Marleau, S.; Ong, H.; Tremblay, A. *Mol. Endocrinol.* **2006**, *20*, 3165–3178.

(10) (a) Collot-Teixeira, S.; Martin, J.; McDermott-Roe, C.; Poston, R.; McGregor, J. L. *Cardiovasc. Res.* **2007**, *75*, 468–477. (b) Febbraio, M.; Silverstein, R. L. *Int. J. Biochem. Cell Biol.* **2007**, *39*, 2012–2030.

(11) For a recent review on growth hormone secretagogues, see: (a) Bowers, C. Y.; Sartor, A. O.; Reynolds, G. A.; Badger, T. M. *Endocrinology* **1991**, *128*, 2027–2035. (b) Korbonits, M.; Goldstone, A. P.; Guerguiev, M.; Grossman, A. B. *Neuroendocrinology* **2004**, *25*, 27–68. (c) Fehrentz, J. A.; Marinez, J.; Boeglin, D.; Guerlavais, V.; Deghenghi, R. I. *Drugs* **2002**, *5*, 804–814.

(12) Demers, A.; McNicoll, N.; Febbraio, M.; Servant, M.; Marleau, S.; Silverstein, R.; Ong, H. *Biochem. J.* **2004**, *382*, 417–424.

(13) Kar, N. S.; Ashraf, M. Z.; Valiyaveettil, M.; Podrez, E. A. *J. Biol. Chem.* **2008**, *283*, 8765–8771.

(14) (a) Gallivan, J. P.; Dougherty, D. A. *Proc. Natl. Acad. Sci. U.S.A.* **1999**, *96*, 9459–9464. (b) Anderson, M. A.; Ogbay, B.; Arimoto, R.; Sha, W.; Kisselev, O. G.; Cistola, D. P.; Marshall, G. R. *J. Am. Chem. Soc.* **2006**, *128*, 7531–7541. (c) Gallivan, J. P.; Dougherty, D. A. *J. Am. Chem. Soc.* **2000**, *122*, 870–874. (d) Searle, M. S.; Griffiths-Jones, S. R.; Skinner-Smith, H. *J. Am. Chem. Soc.* **1999**, *121*, 11615–11620.

(15) (a) Sabatino, D.; Proulx, C.; Bourguet, C.; Klocek, S.; Boeglin, D.; Ong, H.; Lubell, W. D. *Org. Lett.* **2009**, *11*, 3650–3653. (b) Proulx, C.; Lubell, W. D. *Org. Lett.* **2010**, *12*, 2916–2919. (c) Proulx, C.; Lubell, W. D. *J. Org. Chem.* **2010**, *75*, 5385–5387.

(16) (a) Boeglin, D.; Lubell, W. D. *J. Comb. Chem.* **2005**, *7*, 864–878. (b) Melendez, R. E.; Lubell, W. D. *J. Am. Chem. Soc.* **2004**, *126*, 6759–6764. (c) Freeman, N. S.; Hurevich, M.; Gilon, C. *Tetrahedron* **2009**, *65*, 1737–1745. (d) Quibell, M.; Turnell, W. G.; Johnson, T. *J. Chem. Soc., Perkin Trans. 1* **1993**, 2843–2849. (e) Bourguet, C. B.; Sabatino, D.; Proulx, C.; Klocek, S.; Lubell, W. D. *J. Peptide Sci.* **2010**, *16*, 284–296. (f) Bourguet, C. B.; Sabatino, D.; Lubell, W. D. Biopolymers, *Peptide Sci.* **2008**, *90*, 824–831.

(17) Merrifield, R. B. *J. Am. Chem. Soc.* **1963**, *85*, 2149–2154.

(18) (a) Fields, C. G.; Lloyd, D. H.; Macdonald, R. L.; Otteson, K. M.; Noble, R. L. *Pept. Res.* **1991**, *4*, 95–101. (b) Lubell, W. D.; Blankenship, J. W.; Fridkin, G.; Kaul, R. *Sci. Synth.* **2005**, *21*, 713–809.

(19) (a) Agostinis, P.; Goris, J.; Waelkens, E.; Pinna, L. A.; Marchiori, F.; Merlevede, W. *J. Biol. Chem.* **1987**, *262*, 1060–1064. (b) Hanson, S. R.; Whalen, L. J.; Wong, C.-H. *Bioorg. Med. Chem.* **2006**, *14*, 8386–8395.

(20) (a) Escribano, A.; Ezquerra, J.; Pedregal, C.; Rubio, A.; Yruretagoyena, B.; Baker, S. R.; Wright, R. A.; Johnson, B. G.; Schoepp, D. D. *Bioorg. Med. Chem. Lett.* **1998**, *8*, 765–770. (b) Lu, I. L.; Lee, S. J.; Tsu, H.; Wu, S. Y.; Kao, K. H.; Chien, C. H.; Chang, Y. Y.; Chen, Y. S.; Cheng, J. H.; Chang, C. N.; Chen, T. W.; Chang, S. P.; Chen, X.; Jiaang, W. T. A. *Bioorg. Med. Chem. Lett.* **2005**, *15*, 3271–3275. (c) Baker, S. R.; Bleakman, D.; Ezquerra, J.; Ballyk, B. A.; Deverill, M.; Ho, K.; Kamboj, R. K.; Collado, I.; Dominguez, C.; Escribano, A.; Mateo, A. I.; Pedregal, C.; Rubio, A. *Bioorg. Med. Chem. Lett.* **2000**, *10*, 1807–1810.

(21) (a) Chen, C.-G.; Hou, X.-L.; Pu, L. *Org. Lett.* **2009**, *11*, 2073–2075. (b) Ramachandran, P. V.; Madhi, S.; Bland-Berry, L.; Reddy, M. V. R.; O'Donnell, M. J. *J. Am. Chem. Soc.* **2005**, *127*, 13450–13451. (c) Wehbe, J.; Rolland, V.; Fruchier, A.; Roumestant, M. L.; Martinez, J. *Tetrahedron: Asymmetry* **2004**, *15*, 851–858.

(22) (a) Baylis, A. B.; Hillman, M. E. D. *Chem. Abstr.* **1972**, *77*, 34174. (b) Basavaiah, D.; Rao, A. J.; Satyanarayana, T. *Chem. Rev.* **2003**, *103*, 811–891.

(23) Cai, J.; Zhou, Z.; Zhao, G.; Tang, C. *Org. Lett.* **2002**, *4*, 4723–4725.

(24) Madapa, S.; Singh, V.; Batra, S. *Tetrahedron* **2006**, *62*, 8740–8747.

(25) Schwesinger, R.; Willaredt, J.; Schlemper, H.; Keller, M.; Schmitt, D.; Fritz, H. *Chem. Ber* **1994**, *127*, 2435–2454.

(26) Podell, D. N.; Abraham, G. N. *Biochem. Biophys. Res. Commun.* **1978**, *81*, 176–185.

(27) Sieber, P.; Riniker, B. *Tetrahedron Lett.* **1991**, *32*, 739–742.

(28) Sabatino, D.; Lubell, W. D. In *Peptides: Breaking Away (Proceedings of the 21st American Peptide Symposium)*; Lebl, M. , Ed.; American Peptide Society, 2009; pp 58−60.

(29) Kelly, S. M.; Jess, T. J.; Price, N. C. *Biochim. Biophys. Acta* **2005**, *1751*, 119–139.

(30) (a) Bush, C. A.; Sarkar, S. K.; Kopple, K. D. *Biochemistry* **1978**, *17*, 4951–4954. (b) Perzcel, A.; Hollosi, M.; Foxman, B. M.; Fasman, G. D. *J. Am. Chem. Soc.* **1991**, *113*, 9772–9784. (c) Crisma, M.; Fasman, G. D.; Balaram, H.; Balaram, P. *Int. J. Pept. Protein Res.* **1984**, *23*, 411–419.

(31) Rucker, A. L.; Creamer, T. P. *Protein Sci.* **2002**, *11*, 980–985.

(32) (a) Chen, F. M. F.; Kuroda, K.; Benoiton, N. L. *Synthesis* **1978**, *12*, 928–929. (b) Heimer, E. P.; Chang, C. D.; Lambros, T. L.; Meienhofer, J. *Int. J. Pept. Protein Res.* **1981**, *18*, 237–241.

(33) Harigaya, S.; Schwartz, A. *Circ. Res.* **1969**, *25*, 781–794.

(34) Ong, H.; McNicoll, N.; Escher, E.; Collu, R.; Deghenghi, R.; Locatelli, V.; Ghigo, E.; Muccioli, G.; Boghen, M.; Nilsson, M. *Endocrinology* **1998**, *129*, 432–435.

(35) Lee, H. J.; Choi, K. H.; Ahn, I. A.; Ro, S.; Jang, H. G.; Choi, H. S.; Lee, K. B. *J. Mol. Struct.* **2001**, *569*, 43–54.

(36) (a) Lee, H. J.; Ahn, I.-A.; Ro, S.; Choi, K. H.; Choi, H. S.; Lee, K. B. *J. Pept. Res.* **2000**, *56*, 35–46. (b) Andre, F.; Vicherat, A.; Boussard, G.; Aubry, A.; Marraud, M. *J. Pept. Res.* **1997**, *50*, 372–381.